Check for updates

ADVANCED MATERIALS
www.advmat.de

Point-Of-Care Ultra-Portable Single-Molecule Bioassays for One-Health

*Eleonora Macchia, Fabrizio Torricelli, Mariapia Caputo, Lucia Sarcina, Cecilia Scandurra, Paolo Bollella, Michele Catacchio, Matteo Piscitelli, Cinzia Di Franco, Gaetano Scamarcio, and Luisa Torsi**

Screening asymptomatic organisms (humans, animals, plants) with a high-diagnostic accuracy using point-of-care-testing (POCT) technologies, though still visionary holds great potential. Convenient surveillance requires easy-to-use, cost-effective, ultra-portable but highly reliable, in-vitro-diagnostic devices that are ready for use wherever they are needed. Currently, there are not yet such devices available on the market, but there are a couple more promising technologies developed at readiness-level 5: the Clustered-Regularly-Interspaced-Short-Palindromic-Repeats (CRISPR) lateral-flow-strip tests and the Single-Molecule-with-a-large-Transistor (SiMoT) bioelectronic palmar devices. They both hold key features delineated by the World-Health-Organization for POCT systems and an occurrence of false-positive and false-negative errors <1–5% resulting in diagnostic-selectivity and sensitivity >95–99%, while limit-of-detections are of few markers. CRISPR-strip is a molecular assay that, can detect down to few copies of DNA/RNA markers in blood while SiMoT immunometric and molecular test can detect down to a single oligonucleotide, protein marker, or pathogens in 0.1mL of blood, saliva, and olive-sap. These technologies can prospectively enable the systematic and reliable surveillance of asymptomatic ones prior to worsening/proliferation of illnesses allowing for timely diagnosis and swift prognosis. This could establish a proactive healthcare ecosystem that results in effective treatments for all living organisms generating diffuse and well-being at efficient costs.

1. Introduction

"Taking care of the healthy ones" is one of the dreams aimed at creating an efficient system fostering an improved lifestyle for all living species – people, animals, and plants – on our planet. It involves possibly implementing an innovative approach to systematically identify asymptomatic ones as soon as the onset of the illness occurs. Such an approach holds the potential to empower clinicians, phytopathologists, and veterinarians with an advantageous position in the fight against diseases, offering, in principle, significantly better chances for the cure while requiring a much lower budget. Presently, the approach to the cure primarily involves acting when symptoms manifest, resulting in a more reactive sick-care system rather than a proactive health-care one.

In this scenario, the identification of specific biomolecules, for example, proteins and nucleic acids, but also bacteria, and viruses, holds great significance across diverse sectors ranging from public health to environmental concerns, addressing matters related to medicine, food, agriculture,

E. Macchia, M. Caputo
Dipartimento di Farmacia-Scienze del Farmaco
Università degli Studi di Bari "Aldo Moro"
Bari 70125, Italy
F. Torricelli
Dipartimento Ingegneria dell'Informazione
Università degli Studi di Brescia
Brescia 25123, Italy

L. Sarcina, C. Scandurra, P. Bollella, M. Catacchio, L. Torsi
Dipartimento di Chimica and Centre for Colloid and Surface Science
Università degli Studi di Bari Aldo Moro
Bari 20125, Italy
E-mail: luisa.torsi@uniba.it
M. Piscitelli, G. Scamarcio
Dipartimento Interateneo di Fisica
Università degli Studi di Bari Aldo Moro
Bari 70125, Italy
M. Piscitelli, C. Di Franco, G. Scamarcio
CNR IFN
Bari 70126, Italy

The ORCID identification number(s) for the author(s) of this article can be found under https://doi.org/10.1002/adma.202309705

© 2023 The Authors. Advanced Materials published by Wiley-VCH GmbH. This is an open access article under the terms of the Creative Commons Attribution License, which permits use, distribution and reproduction in any medium, provided the original work is properly cited.

DOI: 10.1002/adma.202309705

Table 1. Oligonucleotide DNA and RNA and protein biomarkers targeting progressive diseases along with the fluid in which they can be assayed.

Disease	DNA, RNA	Proteins	Fluid(s) Assayed
Brest Cancer	PIK3CA, TP53, PTEN, AKT1	CA-125, HGF, Myeloperoxidase, OPN, Prolactin)	Blood plasma[7]
Colorectum Cancer	KRAS, TP53, APC, PIK3CA, FBXW7, NRAS, BRAF	CEA, HGF, Myeloperoxidase, OPN, Prolactin	Blood plasma[7]
Esophagus Cancer	TP53, APC	CEA, HFG, TIMP-1, Myeloperoxidase, OPN, Prolactin	Blood plasma[7]
Liver Cancer	TP53, CTNNB1, PIK3CA	CEA, HGF, Myeloperoxidase, OPN, Prolactin	Blood plasma[7]
Ovary Cancer	TP53	CA-125, CEA, Myeloperoxidase, OPN, Prolactin	Blood plasma[7]
Pancreas Cancer	KRAS, GNAS, TP53	CA-125, CA19-9, CEA, CD55, MUC1, HGF, Prolactin, OPN	Blood plasma[7,8]
Stomach Cancer	TP53, PIK3CA, CTNNB1, APC, PPP2R1A	CA15-3, TIMP-1, Myeloperoxidase, OPN, Prolactin	Blood plasma[7]
Lung Cancer	TP53, CDKN2A, PIK3CA, EGFR	CD44, Myeloperoxidase, OPN, Prolactin	Blood plasma[7]
Alzheimer's disease	miRNA miR-501-3p,	hsCRP, IL-1b, scD40L, sTNFR1, sTNFR2, α1-acT, IL-6, Aβ peptides, Tau proteins: tau, p-tau-181, Neurofilament light protein	Blood serum, saliva[6,9,10]
Parkinson's disease	microRNAs, miR-7 and miR-153	PTX3, YKL-40, CRP, sVCAM-1, NLRP3, IL-1β, sTREM2	Blood plasma, blood serum[5,11]
COVID-19	Gene targets, RdRp, N2,E	Spike (S1), envelope (E), and nucleocapsid (N) proteins	Blood serum, Saliva, swab[12,13]
HIV-1	HIV-1 RNA	p24 antigen	Blood serum[14,15]
Influenza virus A and B	Viral RNA	Hemagglutinin (HA), His-Tag	Nasal swab[16]
Xylella Fastidiosa	16S rRNA-processing RimM protein gene coding	IgG of Xylella fastidiosa subsp. pauca strain CoDiRO (strain CFBP 8402)	Olive sap[17]

and veterinary practices. Given the roles played by these biomolecules and pathogens and their impact on population well-being, food security, and ecological soundness, there is an unprecedented need for advanced detection methods that can achieve early, highly sensitive detections.

The elicited biomolecules, generally addressed as "Biological markers or biomarkers", "are measurable indicators that reveal the presence, or the severity of a given disease condition. By definition, they encompass "cellular, biochemical, or molecular changes in cells, tissues, or fluids that can be quantified and assessed to indicate normal biological processes, disease-related processes, or the response to a therapeutic treatment.[1] The term "biomarkers" has now expanded to encompass biological features that can be assessed and analyzed to serve as indicators of regular biological functions, disease-related processes, or responses to medical treatments.[2] The class of biomarkers here discussed is referred to as "molecular biomarkers".[3] This category of molecules offers prodromal indications that they can be detected and utilized at the very early stages of a disease, enabling timely diagnosis through the analysis of peripheral body fluids such as saliva, mucus, serum, plasma, urine, but also olive sap, and others.

Among these, oligonucleotide-based strands (DNA, RNA, mRNA) and proteins/antigens are the most widely used molecular markers.[2,4–6] Their selective binding (capturing) is achieved through biological recognition elements attached at a transducing interface. Oligonucleotides selectively bind to complementary sequence-specific probes, while proteins or antigens are captured by specific antibodies.

In the case of pathogens, their genomic RNA content can be targeted with a probe, or they can be detected with antibodies that recognize proteins on their membrane or capsid. No sample pre-treatment is necessary in the latter case, as the proteins are readily accessible. On the other hand, sample pre-treatment is required to release the genomic material when targeting the genomic pathogen content.

Biomarkers serve purposes such as identifying asymptomatic individuals, characterizing the different stages of progressive disease (induction, latency, and detection) with high precision, as well as serving as targets in clinical trials. The addressing of progressive diseases generally includes not only tumoral conditions but also neurological pathologies as well as viral or bacterial infections. As anticipated, either the pathogen itself is assayed directly, or its genomic content. In **Table 1** some examples of molecular biomarkers that can be found in peripheral biofluids for different diseases are given. Here, communicable and non-communicable diseases are targeted, as both could potentially highly benefit from fast/early diagnosis. While for communicable diseases, this is quite straightforward, swift diagnosis of non-communicable diseases is crucial for improving treatment outcomes and patient well-being. Early detection, particularly in conditions like cardiovascular diseases, diabetes, and certain cancers, facilitates timely interventions, enhancing the chances of successful treatment and preventing disease progression. This proactive approach not only could benefit individual patients but also holds the potential to align with broader public health goals, reducing the prevalence and impact of non-communicable diseases in communities.

A highly convenient and remarkably successful approach that is based on biomarkers detection, to achieve early diagnosis of progressive diseases is the so-called "liquid biopsy".[18–22] Initially developed for the screening of tumors, it is now emerging as a well-established approach with proven effectiveness in prognosis, diagnosis, and monitoring that can be applied to several

© 2023 The Authors. Advanced Materials published by Wiley-VCH GmbH

15214095, 0, Downloaded from https://onlinelibrary.wiley.com/doi/10.1002/adma.202309705 by Universita Di Brescia, Wiley Online Library on [22/01/2024]. See the Terms and Conditions (https://onlinelibrary.wiley.com/terms-and-conditions) on Wiley Online Library for rules of use; OA articles are governed by the applicable Creative Commons License

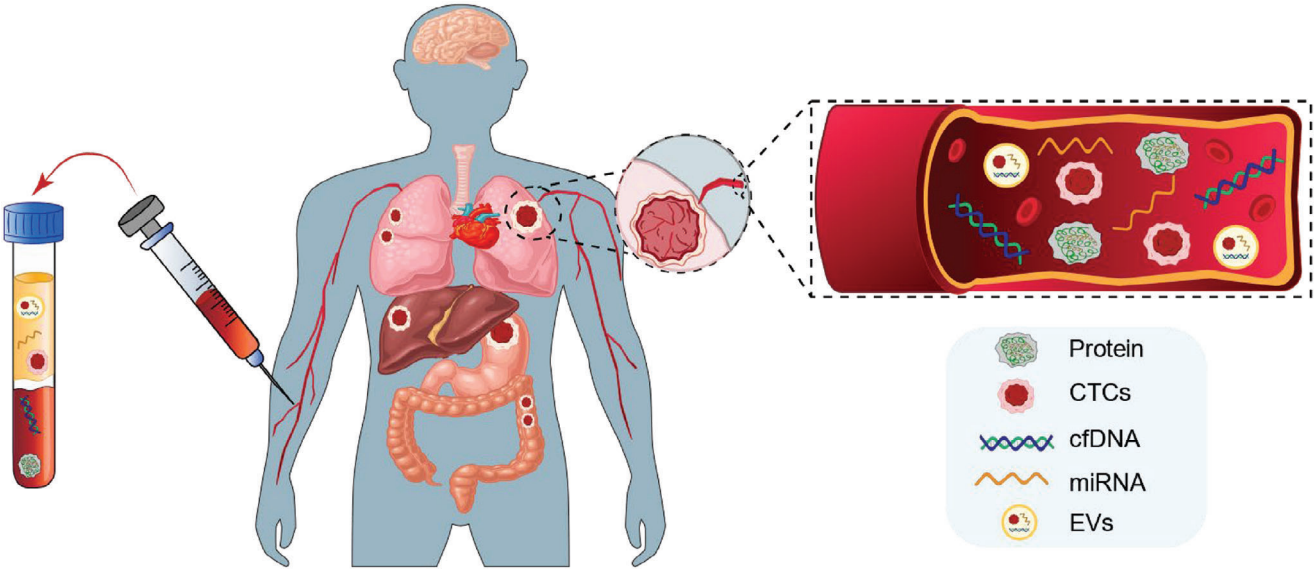

Figure 1. Illustration of the liquid biopsy basic concept. In the central human silhouette, several tumoral lesions are shown in dark red, while a tumoral mass with its vascularization is shown on the top right. These vessels connect the tumoral mass to the main bloodstream. The liquid biopsy starts from the extracted peripheral blood as depicted on the left, which, being connected with the tumoral tissues, comprises a variety of tumorous constituents, such as tumor cells (CTCs), cfDNA, EVs, and miRNA, as schematically shown on the right. Isolation of these components enables the detection of diverse tumor-associated anomalies associated with both the mutations of oligonucleotides and proteins.

other pathologies.[7] In **Figure 1** a schematic representation of the rationale at the basis of liquid biopsy is provided. The tumor mass is here shown as connected with a patient blood stream in which elements such as extracellular vehicles (EVs), microRNA (miRNA), circulating tumor cells (CTCs), circulating cell-free DNA (cfDNA), can be found. Tumors related proteins are also featured as they are becoming more and more important biomarkers.[4,23–25]

Cancer diagnosis is generally accomplished by inspecting the tissues along with the fluids localized where the tumor has developed, and many localized cancers can be still very effectively treated with surgery. Direct tissue biopsy can be, however, invasive and challenging to be repeated as the disease progresses or to check the effectiveness of therapeutic interventions. Moreover, it is critical to diagnose cancer before metastasis occurs.[26] A systematic comparison of the advantages and disadvantages of liquid versus tissue biopsy is a useful exercise to underscore the advancements that liquid biopsies have achieved in the last decade, surpassing the benefits of traditional invasive surgical techniques. One general important aspect concerns the procedures for obtaining a sample, typically involving a minute tissue segment for tissue biopsies and a blood sample for liquid biopsies. The list of liquid biopsy advantages encompasses: being minimally invasive, requiring shorter times, being highly sensitive, requiring lower costs for sample isolation, enabling continuous monitoring of a tumor or a pathology evolution as well as of the response to therapeutic/pharmacological treatment, capable of revealing the spatial-temporal tumor or disease evolution.[25]

In this scenario, assaying for specific tumor biomarkers directly in a peripheral and easily accessible body fluid, as is typical in a liquid biopsy, can be convenient and effective. Besides the circulating tumor cells and their genomic content released upon cell death, also proteins produced by the tumor cells can be found and the interest in detecting them is growing. These proteins can display tissue-specific attributes while retaining their normal structure, harboring mutated regions, or bearing abnormal secondary modifications. However, the concentration of the target biomarkers circulating in such peripheral fluids is much lower than closer to the tumor mass. It can be estimated that a patient affected by cancer at the early stage can have a mutated DNA strand in each mL of blood, which turns into a concentration of 10^{-21} mole L^{-1} (zeptomolar, zM).[27] The presence of mutated proteins is also extremely diluted being lower than 10^{-15} M (femtomolar, fM) concentration.[3,28] Very few immunometric platforms can actually operate at such extremely low concentrations (vide infra).

Biological markers are analyzed using various platforms capable of targeting proteins and oligonucleotides. Among these, two prominent methods are the enzyme-linked immunosorbent assay (ELISA)[29] the gold standard for immunoassays, and the polymerase chain reaction[30] (PCR)-based platforms, which are employed for detecting DNA and RNA markers. Noteworthy advancements in this field include their "digital" evolutions[31] resulting in techniques such as the single-molecule assay (SIMOA)[32,33] and next-generation sequencing (NGS).[34] All these platforms are already commercially available and have been widely adopted, making significant contributions to the integration of biomarker-based diagnostic approaches into everyday clinical practice. While, a comprehensive analysis of these platforms goes beyond the scope of this review, as they notably necessitate voluminous apparats and are consequently unsuitable for point-of-care testing (POCT) applications, for the sake of completeness, small footprint benchtop versions of the SIMOA and the PCR-based technologies are reviewed in **Section 5**.

The aim of this work is to critically review ultra-portable, handheld, and lateral flow technologies for POCT. This is to explore

© 2023 The Authors. Advanced Materials published by Wiley-VCH GmbH

15214095, 0, Downloaded from https://onlinelibrary.wiley.com/doi/10.1002/adma.202309705 by Universita Di Brescia, Wiley Online Library on [22/01/2024]. See the Terms and Conditions (https://onlinelibrary.wiley.com/terms-and-conditions) on Wiley Online Library for rules of use; OA articles are governed by the applicable Creative Commons License

devices that can be as practical and useful as a glucometer[35] and can detect protein and nucleic acid markers at the single-molecule detection limits assuring at the same time high reliability in terms of diagnostic sensitivity and diagnostic selectivity that should be ideally better than 95–99%. Hence the focus is on scrutinizing a couple of promising POCT, single-molecule technologies such as the clustered regularly interspaced short palindromic repeat (CRISPR),[36–48] and the single molecule with a large transistor (SiMoT) both as single-sensor and as a 96 multiplexing array.[8,13,49–51] Among others, these are technologies that can be addressed – by just changing the recognition element, for example, the capturing antibody (to target a specific antigen/protein) or the probe (to bind a specific oligonucleotide) integrated into the disposable accessory cartridge – a large number of different diseases. While CRISPR-based assays, combined with enzymatic amplification, target a single oligonucleotide biomarker,[36] SiMoT can assay at a comparable performance level, both proteins and oligonucleotides. It will be shown how such technologies, resembling a glucometer, can detect a single or few biomarkers in a reliable fashion using a fast, handheld portable device complemented by disposable and feasibly cost-effective cartridges that are customized for each specific application. The technologies here reviewed, which are among the most promising and able to detect a few molecules being also handheld, can be used to possibly diagnose diseases not only in humans but also in plants and animals. They are also in principle ideal for facing the well-being of humans intended as closely linked to the health of animals and the environment. Indeed, diseases can spread between animals and humans (zoonotic diseases), and environmental factors can also impact the health of both. By understanding and addressing these connections, the one-health approach aims to improve disease prevention, surveillance, and control, as well as promote overall health and well-being for all living beings and the ecosystems they inhabit. Finally, both CRISPR-based and SiMoT are prospectively valuable devices to be used in least-developed countries and in low-resource settings to face health crises ranging from epidemics/pandemics to non-communicable diseases.

This Review is organized as follows: in Section 2, we delve into the visionary aspects of one-health point-of-care screening platforms, exploring the potential impact on healthcare delivery and outcomes. Section 3 critically examines the challenge posed by reliably detecting a single or few molecules in 0.1 mL, addressing the intricacies and advancements in molecular diagnostics. Moving forward to Section 4, the focus shifts to the indispensable role of statistical analysis in ensuring the reliability of highly sensitive and selective bioassays, shedding light on the methodologies employed in this critical domain. Section 5 provides an exploration of a couple of the most promising point-of-care assays. In Section 6, we push the boundaries toward their limits, spotlighting a couple, among the few currently available POCT assays (both up to technology readiness level 5), that reliably operate at the single/few-molecules detection threshold. This emphasizes their potential to revolutionize diagnostic precision, showcasing advancements poised to reshape the landscape of point-of-care testing. The vision of a one-health point-of-care screening platform also faces criticisms. Session 7 duly reports on studies, often drawing from COVID-19 data, offering critical perspectives on surveillance campaign relevance and the effectiveness of rapid antigen detection tests. They highlight an unclear efficacy in screening asymptomatic individuals and a lack of evidence for surveillance purposes. Improved antigenic tests and robust trials, suggesting a re-evaluation of current recommendations are also advocated. Finally, Section 8 concludes the examination, summarizing key findings and opening a window into prospects for advancements in ultra-sensitive point-of-care diagnostics.

2. The Vision for a One-Health Point-Of-Care Screening Platform

The vision of a system that caters to maintaining the health of individuals, but also animals, and plants can be exemplified by the scenario presented in **Figure 2**. It is envisioned that the patient is at home maybe sited in a relatively inaccessible and remote location, engaging in self-sampling of saliva, or collecting a small blood sample through a finger prick.

Alternatively, the scenario might involve farmers collecting urine samples from animals or sap samples from plants or trees. The obtained fluid is directly placed onto a cost-effective, disposable cartridge, as illustrated schematically in the figure by showing, by virtue of an example, the bioelectronic SiMoT cartridge.[13] This accessory cartridge is connected to the SiMoT palmar electronic reader device resembling a glucometer device. This reader can be connected to a smart device (a tablet, a smartphone, or a laptop) via Bluetooth or USB, which collects and transfers the data to a cloud platform. Here, an artificial intelligence algorithm automatically analyses the data, and the validated end results are relayed back to the patient's smart device. A similar scenario can be depicted also for a lateral flow[52] device that is based on the CRISPR principle although connectivity for these systems is generally still lacking.

A way to turn such an idealistic one-healthcare ecosystem into a reality is to conduct a thorough screening of the general population (in fact of all the living organisms) using POCT technologies. In fact, early screening is a cornerstone of preventive medicine that improves the chances of successful treatment and enhances overall well-being.[53–55] In this respect, it is essential to find positive cases in primary (before the symptoms appear) or secondary (early or prodromal evaluation) prevention. More in detail it could lead to a higher treatment success rate of many diseases, including cancer, cardiovascular conditions, and diabetes. Treatment options are in fact often more effective and less invasive at early stages, leading to improved patient outcomes. It could also lead to reduced disease progression as detecting and intervening in the early stages of a disease can prevent its progression to more advanced and severe stages. This can help minimize damage to tissues, organs, and overall health. Another advantage is the lower healthcare costs because early screening can lead to more cost-effective healthcare. Treating diseases at advanced stages often requires more extensive and expensive interventions, hospitalizations, and therapies. Early detection and treatment can help reduce these costs. An improved quality of life is another advantage as timely detection and treatment can help individuals maintain a better quality of life. Addressing health issues early can also prevent complications and reduce the impact of symptoms on daily activities. Screening is also key in the prevention of the spreading of infectious diseases. Identifying and isolating infected individuals early can help contain outbreaks and

© 2023 The Authors. Advanced Materials published by Wiley-VCH GmbH

15214095, 0, Downloaded from https://onlinelibrary.wiley.com/doi/10.1002/adma.202309705 by Universita Di Brescia, Wiley Online Library on [22/01/2024]. See the Terms and Conditions (https://onlinelibrary.wiley.com/terms-and-conditions) on Wiley Online Library for rules of use; OA articles are governed by the applicable Creative Commons License

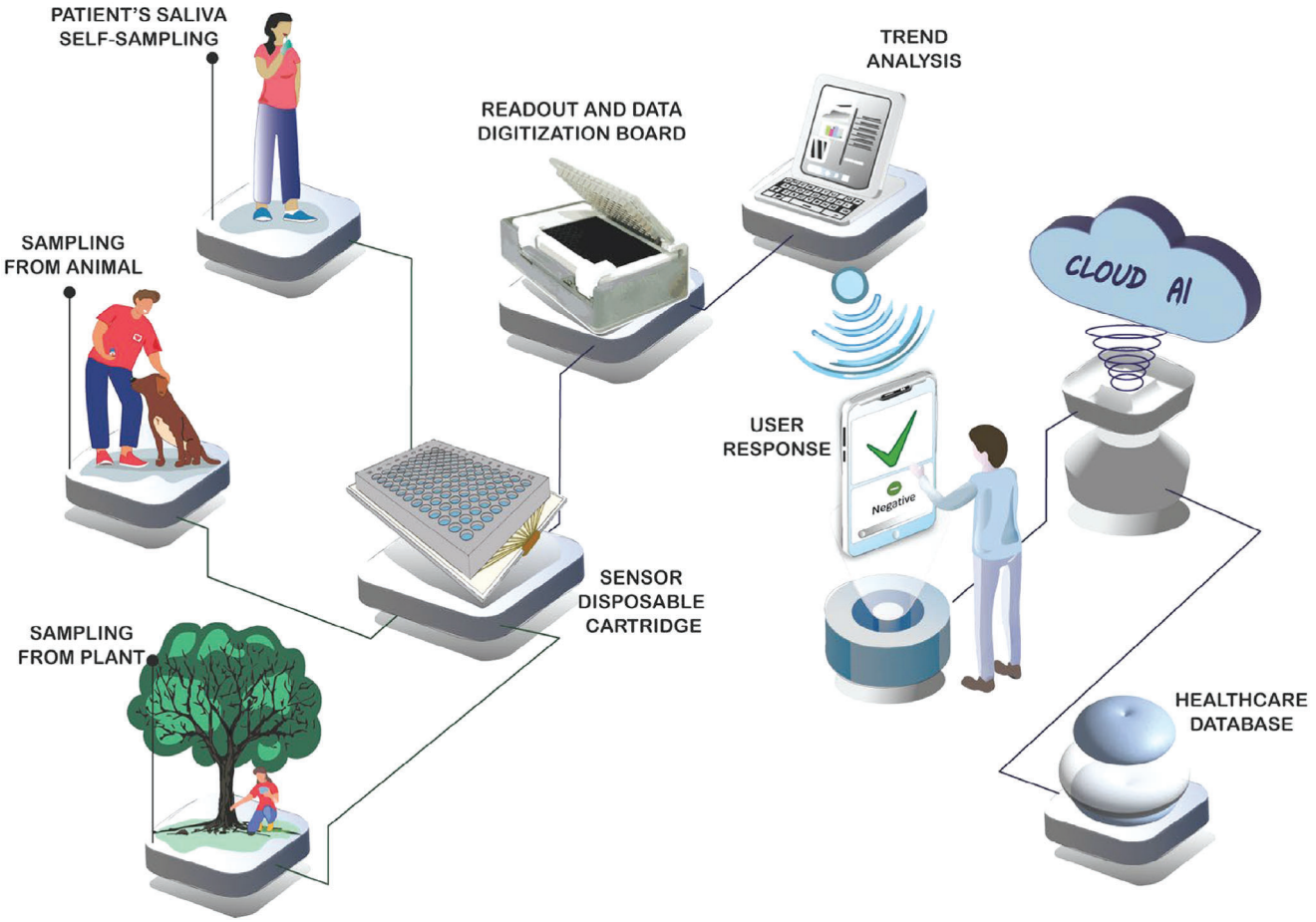

Figure 2. The vision of the screening with a POCT technology in a one-healthcare ecosystem.

protect public health. Finally, it can foster health equity because early screening can contribute to reducing health disparities by ensuring that individuals from all backgrounds have access to timely and effective healthcare. Finally, ethical issues associated with the use of biomarkers-based tests should be mentioned. For instance, most healthcare systems require that those who test positive, even if they do not show symptoms, undergo some follow-up tests and treatments that should be available for all.

POCT technologies, that provide immediate results enabling faster decision-making at the individual level, are key to implementing a successful screening of a cohort. This is why the World Health Organization has recommended several criteria that should be met by an ideal POCT technology. These criteria, addressed with the "REASSURED"[56,57] acronym, are based on the earlier 2003 "ASSURED" set.[57] According to ASSURED an ideal POC test technology, should encompass: Affordability – POCTs should be cost-effective to make them accessible across various healthcare settings. Low manufacturing costs and minimal additional equipment are important factors. Sensitivity – the test should have a high level of accuracy and sensitivity, enabling reliable detection of a marker also at low concentrations. Specificity – false positive (vide infra) results should be minimized. The goal is to achieve a level of sensitivity and specificity in POCT diagnostics that closely resembles that of laboratory-based assays. This ensures that the POCTs are adept at correctly identifying true positive cases (vide infra) while simultaneously minimizing the occurrence of false positives (vide infra). User-friendliness: The technology should be easy to use and require minimal training to operate. Simple instructions and intuitive interfaces are crucial, especially in settings with varying levels of expertise. Rapid Results with a Robust system – A POCT technology should provide quick results within a short time frame, ideally within minutes to a few hours. This is essential for immediate decision-making and patient management. The system should also be robust enough to withstand variations in environmental conditions, such as temperature and humidity, especially in settings with limited infrastructure. Equipment-free – Portability is vital for POCTs to be used in various locations, including remote or resource-limited areas. They should also be compact, lightweight, and handheld devices. Deliverable to end-users – or data connectivity meaning integration with digital platforms and connectivity to electronic health records to facilitate data management, analysis, and reporting. The "REASSURED"[56] revised set of criteria adds: Real-time insights into the strategies to control a disease augment the Effectiveness of a healthcare system, and eventually elevate patient outcomes. Other relevant aspects are also: minimal sample requirements – the test should require a small volume of sample, such as blood, saliva, or urine, to

© 2023 The Authors. Advanced Materials published by Wiley-VCH GmbH

15214095, 0, Downloaded from https://onlinelibrary.wiley.com/doi/10.1002/adma.202309705 by Universita Di Brescia, Wiley Online Library on [22/01/2024]. See the Terms and Conditions (https://onlinelibrary.wiley.com/terms-and-conditions) on Wiley Online Library for rules of use; OA articles are governed by the applicable Creative Commons License

minimize discomfort for patients and simplify sample collection; versatility – adaptable to detect multiple analytes or pathogens to enhances its utility in different clinical scenarios; stability – the reagents and components used in the test should be stable and have a reasonable shelf life, ensuring reliable results over time; embedded quality control – incorporation of internal controls and quality assurance measures ensures the reliability and consistency of test results; regulatory approval – the technology should meet regulatory standards and obtain necessary approvals for safety, efficacy, and accuracy; scalability – POCT technologies should be scalable for mass production and distribution to accommodate large-scale testing needs, such as during outbreaks or pandemics; diagnostic range – the technology should cover a wide diagnostic range, from early detection to monitoring disease progression and treatment response; and last but not least assure global accessibility – the technology should be accessible to diverse populations worldwide, addressing the healthcare needs of both developed and developing regions.

A further important element is the integration of POCT screening with the "one-health" method that takes into consideration the health interrelations among humans, animals, and the environment. For instance, one-health principles may guide the screening of individuals who have been exposed to animals or environments where zoonotic diseases are prevalent. It could also be of relevance in epidemiological surveillance of disease patterns in humans, animals, and the environment. Screening programs could be established to monitor the emergence of zoonotic diseases or detect outbreaks that have the potential to spread across species. Also relevant is the monitoring of wildlife populations.

3. The Challenge of Reliably Detecting a Single Molecule in 0.1 mL

Detecting a single biomarker within a droplet of peripheral biofluid is crucial to conveniently enable accurate early diagnosis, as envisioned in a liquid biopsy-type assay. A droplet, equivalent to ≈0.1 mL, represents the minimal quantifiable volume that can be dispensed by using a standard pipette certified by the manufacturer with a precision of 1%. Within 0.1 mL, the presence of a single biomarker yields a target molecule concentration of 10^{-20} zeptomolar (zM), which is essentially the lowest possible concentration also addressed as the "physical limit" in biomarkers detection. This concentration entails, in fact, both the smallest number of markers (one) within the minimal volume that can be reliably processed out of a conventional laboratory framework. Assuming that the volume of a protein is $\approx(10\ \text{nm})^3 = 10^{-21}$ L, it will occupy one of the 10^{17} protein-sized volumes available in 0.1 mL.

Working with a precisely measured 0.1 mL volume ensures minimal error across various procedures, such as the sequential dilution process, which is essential in an assay. Here, the concentration error at each dilution step (from the mother down to the 10^{-20} zM solution) remains consistently at 1%, up until the point where the Poisson sampling error must be considered.[13] This error is quantified by the square root of the particle count within the sample, and it surpasses 1% when the particle count in 0.1 mL falls below 10 000 particles. This translates to a concentration of $\approx 2 \times 10^{-17}$ M or 20 attomolar (aM).

These considerations lay the groundwork for understanding why single molecule detections are influenced by two interconnected issues: diffusion barrier and low signal-to-noise ratio. The diffusion barrier issue[58,59] refers to the challenge for an individual molecule to reach the transducing interface by Brownian random diffusion in a volume (0.1 mL) that is 10^{17} times larger than the molecule itself. The time needed to hit a capturing interface generating the signal to be transduced, can be unfeasibly high, particularly if the area of the detecting interface is nanometric in size. By virtue of an example, let's consider a protein to be captured by one of its cognate antibodies attached to a transducing interface, for example, the gate of a transistor or a plasmonic interface. The time needed to hit the interface depends on the concentration of the proteins and the size of the interface. Let's consider a 1 fM concentration protein solution, this means that in 0.1 mL $\approx 10^5$ proteins are present. If the detecting interface is 200 nm wide in diameter, the first protein will hit the interface in a one-day timeframe while it will take a week for 10 proteins to hit the same detecting interface. If the interface is three orders of magnitude larger (200 μm) the first protein will hit the detecting interface in a few seconds while 10 will reach the surface in one minute.[60]

When single molecule detection is performed by a nanometric transducing interface such as for instance nanopores,[61] or nano-plasmonic approaches[62] to overcome the mass transport diffusion barrier, a concentration quite high of the target protein is to be present. It has been proven that one diffusing protein will hit a nanometric interface in a timeframe of minutes, only if they are confined in a volume as small as 1 μm^3 or, equivalently, 1 femtoliter, fL.[32] This means that a protein concentration in the nM range is needed. Under these conditions the nanometric interface can detect a sequence of single binding events, meaning that it can detect at the single molecule resolution. However, it cannot detect a single molecule limit-of-detection in 0.1 mL as this is a too-low concertation being 10^{11} times more diluted than the nM concentration needed.

As already discussed, to reach detection in the 10^{-15} M concentration range, a 200 μm wide surface is needed whose area ($4\ 10^{-8}$ m^2) is at least 10^8 times that of the protein (10^{-16} m^2). Hence, the diffusion limit is overcome when a detecting interface is at least a hundred million times larger than the footprint of the target molecule. In the SiMoT technology single molecule detection is achieved with a surface that is even larger, namely 10^{12} times larger than a typical protein footprint.[49] This is like spotting a single droplet of water falling in a lake that is 1 km wide.

Through a systematic exploration that combines theoretical analysis and experiments, it has been established that the diffusion barrier limit does not pose an obstacle for SiMoT and large-area detecting technologies. A millimeter-sized bioelectronic interface, equipped with trillions of bio-recognition elements, can effectively detect a single molecule within minutes.[58] This assertion is supported by modeling experimental data obtained from SiMoT devices, utilizing Einstein's theory of Brownian diffusion to provide the conditional probability of at least one out of N antigens being in proximity to the gate surface. Assuming random dispersion of N IgG antigens in the assayed volume V, we calculated the probability of one being sufficiently close to the gate surface (within a Δr distance) to potentially collide with it. Notably,

© 2023 The Authors. Advanced Materials published by Wiley-VCH GmbH

15214095, 0, Downloaded from https://onlinelibrary.wiley.com/doi/10.1002/adma.202309705 by Universita Di Brescia, Wiley Online Library on [22/01/2024]. See the Terms and Conditions (https://onlinelibrary.wiley.com/terms-and-conditions) on Wiley Online Library for rules of use; OA articles are governed by the applicable Creative Commons License

with an incubation time of 10 min, we estimated a substantial value of $\Delta r = 37$ µm, consistent with observed sensor responses at various concentrations and incubation times.[58] Importantly, the model suggests that the rapid spinning of the diffusing antigen, covering the entire solid angle in 25 µs, enables the molecule to swiftly orient itself for binding to a capturing element. This study demonstrates that the diffusion barrier challenge, which limits the utility of single-molecule detection at nanometric interfaces for solutions with concentrations below picomolar levels, is overcome when employing a SiMoT-like bioelectronic sensor featuring a micrometric or millimeter-wide detecting interface. In such cases, a single molecule can be detected within a few minutes in a 0.1 mL solution, even with concentrations as low as a few tens of zeptomolar.

However, while a larger interface addresses the diffusion barrier issue, it gives rise to a potentially even more severe problem: the low signal-to-noise ratio. Specifically, the question is whether an event involving a minuscule portion of the detecting interface can produce a detectable signal. In simpler terms, can a signal from a single binding event whose footprint is orders of magnitudes lower than the whole surface stand out from the background noise? The answer is evidently no, and the resolution to this challenge lies in the existence and exploitation of amplification effects that allow for single molecule detections in a larger volume or at an extended interface, as elucidated in Sections 6.1.2 and 6.2.2.

4. Statistical Analysis in Reliable Highly Sensitive and Selective Bioassays

The aim of ultrasensitive biomarker assay technology is to reliably detect a specific marker while maintaining the occurrence of false negatives and false positive errors below 1–5%.[63] A false positive refers to an incorrect result obtained from a diagnostic test, indicating the presence of a condition or disease in an individual who is not affected by it. Although all the errors concur to lower the reliability of an assay, false positives are generally less impactfully. In fact, they can lead in the worst scenario to unnecessary anxiety, additional tests, treatments, or interventions that are not required, and can result in increased healthcare costs, but they are not a threat to a patient's life. They are also less frequent because medical tests are often designed with stricter criteria for successfully reading a positive result. This helps ensure that only cases with a high likelihood of the condition being tested for, are classified as positive. As a result, the threshold for a positive result is set high, reducing the likelihood of false positives. This is particularly true in the case of devices that are not highly precise (high level of random errors). Conversely, under the same conditions, false negative errors are more common and can also pose a threat to a patient's life. In hypothesis testing, a type II error is a statistical concept denoting the mistake made when an incorrect null hypothesis is not dismissed. This situation leads to a false negative outcome, alternatively addressed as an omission error. In the context of medical diagnosis, a false negative refers to an incorrect result in which a test fails to identify a condition or disease that is present in the individual being tested. In other words, the test indicates a negative result (absence of the condition), but this result is inaccurate because the individual does indeed have the condition. False negatives are life-threatening as they can potentially lead to delayed or missed diagnoses, as the individual may not receive the necessary treatment or further evaluation due to the incorrect test outcome. It's a critical concern in medical testing, as minimizing false negatives is crucial for ensuring that individuals who require medical attention receive timely and appropriate care.

The occurrence of these errors forms the basis for defining the figures of merit that characterize the reliability of a diagnostic procedure, namely diagnostic sensitivity, and selectivity. Diagnostic sensitivity is the percentage of true positives (TP) patients with respect to the total number of patients that are tested as positives (P), the latter also including the false negatives (FN), so that P = TP + FN. Diagnostic specificity is the percentage of true negative (TN) patients with respect to those that are tested as negatives (N) that also includes the false positives (FP) so that N = TN + FP; the equations are therefore:

$$\text{diagnosticsensitivity} = \text{TP}/\text{P} = \text{TP}/\left(\text{TP} + \text{FN}\right) \times 100\% \quad (1)$$

$$\text{diagnosticspecificity} = \text{TN}/\text{N} = \text{TN}/\left(\text{TN} + \text{FP}\right) \times 100\% \quad (2)$$

The diagnostic sensitivity, which accounts for false negative errors, quantifies an assay or a protocol ability to correctly identify during screening, the ill ones. The greater the assay's sensitivity, the more comprehensive the identification of affected individuals. However, at the onset of a disease when symptoms are not yet present or are unclear, false positive errors are highly probable. As a patient's health status is further evaluated through follow-up assessments, and as a disease progresses, the patient's true condition becomes increasingly apparent. This reality often makes it exceedingly challenging to have available an assay technology that achieves 100% diagnostic sensitivity during the early stages of a disease. This difficulty underscores the true challenge in point-of-care screening for early diagnosis. Conversely, diagnostic specificity considers false positive errors, in which an unaffected individual is incorrectly diagnosed as positive for a particular condition. This situation is generally less frequent unless the biomarkers lack the needed specificity.

A holistic parameter, denoted as efficiency, is formulated by calculating the geometric mean of both the sensitivity and specificity values:

$$\text{efficiency} = \sqrt{\frac{TP \times TN}{(TP + FN) \times (TN + FP)}} \quad (3)$$

The efficiency can vary between 0 and 1, with 0 representing situations where either sensitivity or specificity is zero, and 1 indicating that both parameters are at 100%. Receiver operating characteristic (ROC) curves are commonly employed as a visual aid for assessing the effectiveness of a particular diagnostic test or biomarker in distinguishing between healthy and diseased individuals.[64] The ROC curve illustrates the correlation between true positives and false positives. ROC curves that approach the diagonal bisector indicate a diagnostic test with weak analytical performance, essentially randomly assigning individuals to the healthy and diseased categories. Conversely, ROC curves that deviate from the diagonal line are associated with an effective diagnostic test. This effectiveness is frequently measured by assessing the area under the curve, which ranges from 0 to a

© 2023 The Authors. Advanced Materials published by Wiley-VCH GmbH

15214095, 0, Downloaded from https://onlinelibrary.wiley.com/doi/10.1002/adma.202309705 by Universita Di Brescia, Wiley Online Library on [22/01/2024]. See the Terms and Conditions (https://onlinelibrary.wiley.com/terms-and-conditions) on Wiley Online Library for rules of use; OA articles are governed by the applicable Creative Commons License

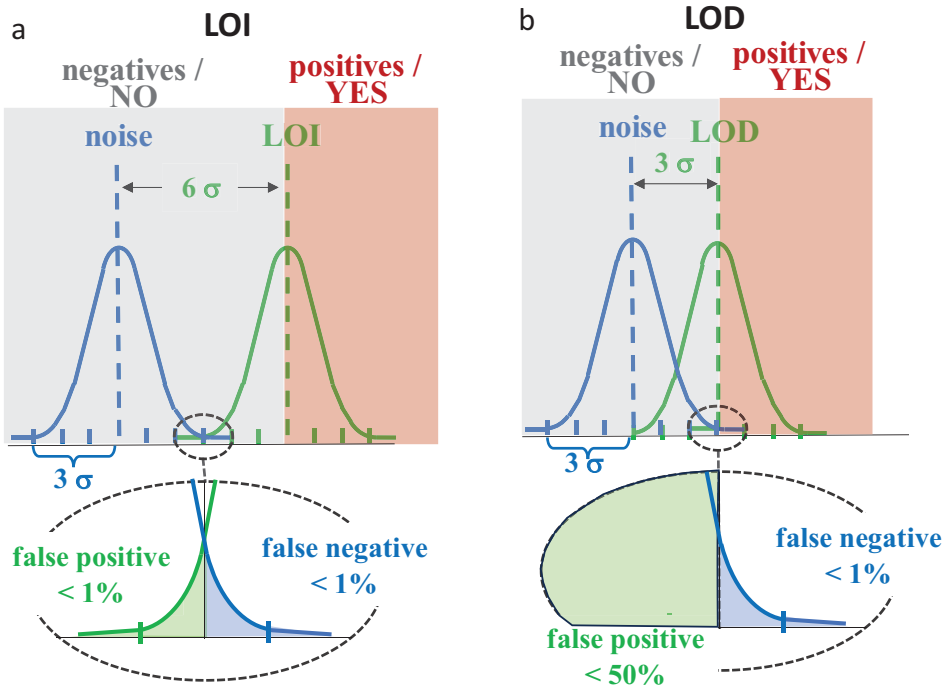

Figure 3. Graphical representation of the Gaussian distribution of the assay random error at the a) LOI level and b) LOD level. The gray and red shaded areas are the fields of the negative (NO) and positive (YES) assay outputs.

maximum of 1 and increases as the diagnostic test's performance improves.

Another important statistical parameter is the threshold at which a specific figure of merit or parameter is established to differentiate between a positive and a negative result. Depending on the choice a different level of statistical confidence will be associated with the data set. For this purpose, the limit of identification (LOI) can be conveniently employed. By definition,[65,66] the LOI quantifies the amount or the lowest concentration of a substance that can be reliably detected and distinguished from the background noise with an incidence of false negatives and false positives that are both below 1%. The LOI is typically determined by conducting a series of measurements to assess the statistical distribution of the random error in a blank or negative control experiment. Those are measurements conducted, ideally, in the same exact conditions as the analysis, but in the presence of no target biomarker or analyte. In **Figure** 3a a graphical representation of the LOI is given. Here the Gaussian blue curve is the distribution of the random error that is measured with the blank or negative control experiment that needs to be reaped several times to hold statistical significance. This sets all the features characterizing the noise of the assay: its average value level (dotted blue line) and its standard deviation, σ, which quantifies the precision of the measurements. The Gaussian curve in green sets the LOI level or else the error distribution at the threshold separating negative and positive values. Its average peak is set at 6 σ from the average of the noise while the σ is kept as that of the blue curve. This is an assumption that is justified only when the negative control experiments and the assay experimental settings are very much alike.

The areas underneath the overlapping parts of the two Gaussian curves assure that when the LOI is taken as the threshold to discriminate a positive output from a negative one, the expected occurrence of both false positives and false negatives is below 1%.

In the case when the threshold is set at 3 σ from the average of the noise (Figure 3b), the level is addressed as a limit of detection (LOD) and the expected occurrence of a false negative is still lower than 1%, while that of false positives is up to 50%. Such a choice becomes necessary when the assay has a very high average level of noise and standard deviation (low precision) as it generally occurs with most commercially available lateral flow strip test POCT technologies whose LOD is, generally, in the range of nM to μM, with best performance level at $\approx 10^{-11}$ M (10 pM).[52] The very high average level of noise is generally, erroneously addressed as "low sensitivity" while in fact, it is to be addressed as high LOD. In analytical chemistry, the sensitivity of an assay is the slope of the calibration curve. In the case when this threshold is set at 9 or even 10 σ higher than the average of the noise, the level is addressed as a limit of quantification (LOQ).

In a quantitative assay, a calibration step prior to each measurement is generally required as obtaining an exceedingly robust and universally applicable mathematical relationship between the measured response and the actual concentration of the analyte in the sample is extremely rare. Moreover, the minimum quantifiable concentration is determined by the LOQ. This ensures that the overlap between the Gaussian distributions of LOD and LOQ is kept to less than 1%. Consequently, this implies that the occurrence of false positives and false negatives in quantification, as compared to mere identification, is guaranteed to be less than 1%.

© 2023 The Authors. Advanced Materials published by Wiley-VCH GmbH

15214095, 0, Downloaded from https://onlinelibrary.wiley.com/doi/10.1002/adma.202309705 by Universita Di Brescia, Wiley Online Library on [22/01/2024]. See the Terms and Conditions (https://onlinelibrary.wiley.com/terms-and-conditions) on Wiley Online Library for rules of use; OA articles are governed by the applicable Creative Commons License

A qualitative YES–NO assay is a type of analytical test used to determine the presence or absence of a particular substance or analyte in a sample, without providing its quantification. Instead of quantifying the amount of the substance, a qualitative assay simply provides a Boolean "YES" (positive or signal-ON) or "NO" (negative or signal-OFF) answer about its presence.[67–69] Qualitative assays are often used in various fields, including chemistry, biology, medicine, and environmental science. These assays can be designed to detect specific molecules, microorganisms, genetic markers, antibodies, or other relevant components in a sample. The goal is to establish whether a particular substance of interest is present or not in the sample assayed, without determining its exact concentration. Some common examples of qualitative assays include pregnancy tests to assay the human chorionic gonadotropin hormone in a woman's urine, indicating pregnancy; pathogen detection with qualitative assays used to identify the presence of a given pathogen, like bacteria or viruses, in blood, saliva, or swabs; drug tests that determine whether specific drugs or their metabolites are present in a person's urine or blood; food allergen testing designed to determine the presence of allergenic substances in food products, helping to ensure food safety for individuals with allergies.

In all these assays selectivity is also assured by the presence of a probe or an antibody that binds only to the target biomarker. In fact, accurate identification of a given oligonucleotide sequence, within a vast majority of normal genetic sequences or of a given antigen, holds growing significance in the realm of clinical disease diagnosis, notably in cancer and other ailments. Numerous methodologies have emerged to address this challenge, with a substantial portion employing targeted binding between the genetic material of interest and ad hoc designed probes. For proteins and pathogens specific monoclonal and polyclonal antibodies serve the scope.

If a qualitative assay engages the LOI as a threshold signal to sort between positive (YES) and negative (NO) data, the occurrence of false positive and false negative errors will both remain below 1%. This leads to diagnostic sensitivity and specificity levels exceeding 99%. Furthermore, in cases where the assay's performance is sufficiently high to permit the setting of the LOI below the output generated by detecting a single biomarker, such a qualitative assay could determine, with a confidence level surpassing 99%, whether a 0.1 mL droplet of fluid contains at least one copy or molecule of a specified marker or pathogen (YES) or not (NO). Among commercial bench-top assay technologies, qualitative real-time PCR methods can assure such a performance level in the detection of oligonucleotide biomarkers.[64]

Achieving selectivity or even specificity is essential, and all the possible effort should be in place to prove that it is accomplished. Selective binding, or capturing, is reached by employing biological recognition elements attached to a transducing interface. Oligonucleotides exhibit specificity as they selectively attach to complementary sequence-specific probes, while proteins or antigens find capture through specific antibodies; the latter selectively also bind viruses and bacteria. The assurance of selectivity in all these assays is hence granted by the existence of a probe or antibody designed to exclusively bind to the target biomarker. The precise identification of a given oligonucleotide sequence, amid a plethora of normal genetic sequences, or of a specific antigen, assumes heightened importance in clinical disease diagnosis, particularly in conditions like cancer. To prove that the assay is selective, critically important is to properly design negative control experiments. As we have seen the LOI is usually established through a series of measurements aimed at evaluating the statistical distribution of random errors in a blank or negative control experiment. These measurements are ideally carried out under precisely the same conditions as the analysis but in the absence of any target biomarker or analyte. Hence, while assessing the level of the LOI it is also assessed a given assay level of selectivity.

5. Examples Taken Among the best Performing Point-Of-Care Testing Assays

Before delving into the specifics of the selected technologies that share the unique capability of detecting at a LOD or even at a LOI a single marker while being also either handheld or a lateral flow strip test – all while maintaining full accountability as POCT technologies – let's provide an overview of the landscape of the most effective and performing POCT assays, though they are not capable of reaching single molecule detections. In **Figure 4** some of the most relevant commercially available POCT strip tests, handheld devices, and portable and small footprint bench-top systems technologies are featured. In **Table 2** these commercially available technologies are assessed against the REASURRED main figures of merit. The SiMoT and CRISPR/Cas, which are not commercially available yet, will be duly illustrated in the next section.

As it is apparent a great deal of POCT technologies is now commercially available and here only a few are reviewed. They can measure several critical parameters. After the Covid pandemics, many surveillance test technologies to detect extremely low concentrations of DNA and RNA biomarkers can be found that are highly performing and reliable. They can show very low LODs with the Abbot ID Now[77] and the SIMOA[80] ones being among the best performing. All the technologies proposed show excellent diagnostic sensitivity and selectivity. Moreover, they are very fast and generally easy to use. Worth to note is that the only available technology for immunoassay is the SR-X SIMOA by Quanterix which can perform multiplexing assays of many proteins and antigens at extremely low concentrations in a highly reliable fashion. For instance, ELISA assay limitation is overcome by the SIMOA[83,84] technology which is based on paramagnetic beads functionalized with capturing antibodies that can assay antigens/proteins, by confining an individual enzyme and its fluorogenic molecular-substrate into an fL-large volume. With this very effective strategy LODs below fM (reaching down to 220 zM, for example, 10–10^5 molecules in 0.1 mL) have been proven.[84] A faster and more practical SIMOA platform called planar technology (SP-X Imaging and Analysis System),[32,85] it's very convenient but it can operate only at higher LODs.[86] Last but not least very relevant are also some of the top-performing POCT handheld assays such as Cue Health (USA)[73] and PEBBLE by Biopix Dna Technology P.C. (Gr) for molecular tests,[74] along with LumiraDx (UK) for immunoassay.[75]

6. POCT Assays Performing at the Single-Molecule Limit

This section highlights a couple of POCT technologies known for their commendable reliability, ultra-portability, and capability

© 2023 The Authors. Advanced Materials published by Wiley-VCH GmbH

15214095, 0, Downloaded from https://onlinelibrary.wiley.com/doi/10.1002/adma.202309705 by Universita Di Brescia, Wiley Online Library on [22/01/2024]. See the Terms and Conditions (https://onlinelibrary.wiley.com/terms-and-conditions) on Wiley Online Library for rules of use; OA articles are governed by the applicable Creative Commons License

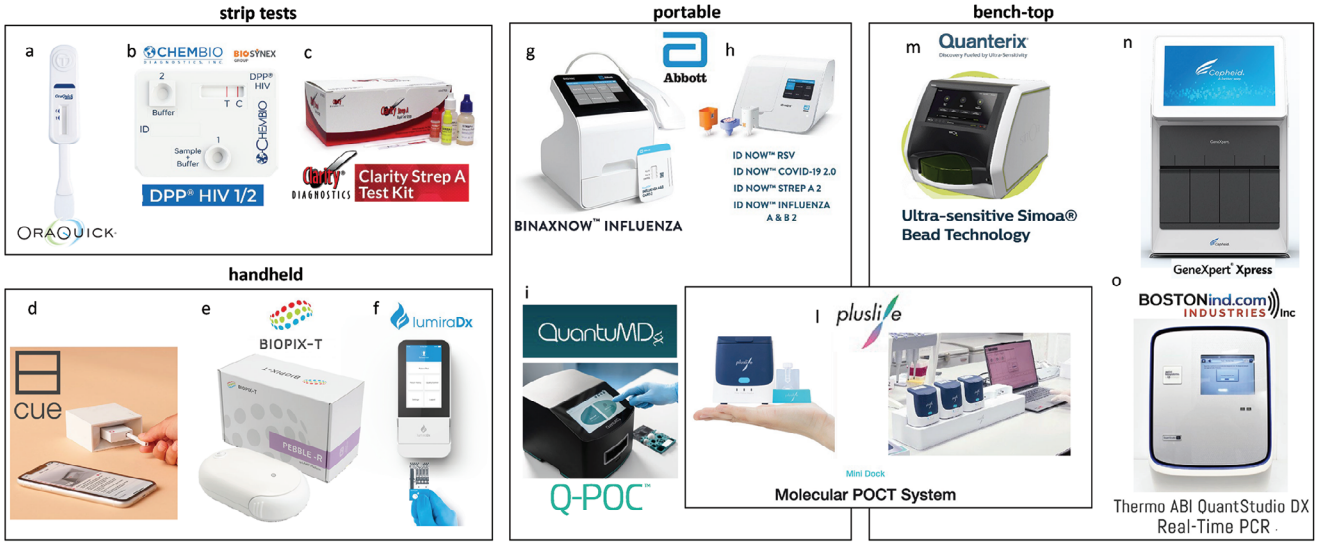

Figure 4. a) OraQuick Rapid HIV Test[70] is a handheld test that detects HIV antibodies in oral fluid, providing results within 20 min. Used with permission from Oraquick. b) Chembio DPP HIV 1/2 Assay[71] assays HIV-1 and HIV-2. Used with permission from Chembio Diagnostics c) Clarity Strep A Test[72] is a rapid test detecting streptococcal infections (strep throat). Used with permission from Clarity Diagnostics. d) Cue Health's molecular test[73] is a rapid POC nucleic acid amplification-based test authorized by the US Food and Drug Administration for point-of-care use to detect SARS-CoV-2. Used with permission from Cue Health Inc. e) PEBBLE[74] by Biopix Dna Technology P.C. is a compact device for performing real-time colorimetric LAMP (qcLAMP) that offers molecular rapid detection of infectious diseases (such as COVID-19 and Influenza A) in saliva, nasal or pharyngeal swab specimens. f) LumiraDx[75] is a portable diagnostic device that provides rapid results for a range of critical tests using blood, urine, nasal and vaginal specimens. Used with permission from LumiraDx g) BinaxNOW Influenza Test[76] is a rapid influenza diagnostic test that provides results within 15 min. h) Abbott ID NOW[77] is a rapid molecular diagnostic platform designed to provide quick and accurate results for various infectious diseases. i) Quantum MD Q-POC[78] is also a platform for a swift multiplex PCR testing system that provides, precise, and actionable outcomes in ≈30 min. Used with permission from QuantuMDx Group Ltd l) Pluslife – Molecular POCT System[79] is a portable molecular diagnostic system used for detecting various infectious diseases, including tuberculosis and COVID-19; it comes either as a single sensor handheld device or as an eight-channel dock system where parallel analysis can be performed. m) SR-X SIMOA – Quanterix[80] is a benchtop system for multiplex immunometric detections for many antigens. n) Cepheid GeneXpert[81] combines PCR-based detection with the single integrated cartridge to diagnose a range of infections, including respiratory infections, sexually transmitted diseases, tuberculosis, and more. Used with permission from Cepheid o) Thermo ABI QuantStudio DX Real-Time PCR 4 470 660[82] system can identify alterations in gene expressions as subtle as a 1.5-fold change for the assessment of gene expression, microRNAs, noncoding RNAs, variations in gene copy numbers, drug metabolism enzymes, and levels of protein expression.

for single-molecule detection at the LOD or LOI level. Notably, these technologies have progressed to technology readiness levels 5–6, indicating validation in a relevant environment with pre-clinical studies underway,[87] although commercialization is still pending. Two illustrative examples chosen for discussion are CRISPR-Cas (Cas being a specific protein involved in the CRISPR process), where single-molecule detection is achieved in conjunction with enzymatic amplification, and SiMoT. In **Figure 5** the two technologies are featured, while in **Table 3** the performance level of some of the best-performing systems is schematically summarized.

In the following, some of these single-molecule POCT technologies are reviewed in depth and their performance levels will be illustrated with several examples.

6.1. CRISPR/Cas Bioassay in a Nutshell

CRISPR/Cas biosensing is a technique that utilizes the precision of the CRISPR/Cas gene editing system to detect specific oligonucleotide sequences in a sample. The method leverages the natural ability of CRISPR to identify and target specific genetic sequences of the genome of an organism or a biomarker, and it has been adapted for various diagnostic and detection purposes. A CRISPR/Cas-based bioassay starts with the target DNA sequence recognition that involves a Cas protein and a guide RNA encompassing two strands. One of the two RNA strands is engineered to be complementary to the target DNA. The engineered Cas protein and guide RNA are introduced into the sample containing the genetic biomarker or the pathogen to be detected. The RNA guides the Cas protein to bind to the complementary sequence and upon binding the gene-editing cleavage activity elicits a conformational change in the Cas protein. This triggers a signal, such as a fluorescent or color change, which indicates the presence of the target sequence. In this regard, many examples of CRISPR/Cas biosensing platforms without pre-amplification steps have been explored reporting the limit of detection in the range of fM–nM.[96–98]

To reach single molecule detections, the CRISPR/Cas biosensing system is complemented by a molecular amplification step as a reliable optical/colorimetric detection of a single DNA copy in 0.1 mL is not possible. As a matter of fact, if in 0.1 mL there is a sufficiently high number of CRIPSR-Cas systems, and a "label" is present (for instance a florescent element) the single sparkling generated upon binding will occur in a 10^{-17} fraction of the sampled droplet and this is a too weak signal to be discriminated

© 2023 The Authors. Advanced Materials published by Wiley-VCH GmbH

15214095, 0, Downloaded from https://onlinelibrary.wiley.com/doi/10.1002/adma.202309705 by Universita Di Brescia, Wiley Online Library on [22/01/2024]. See the Terms and Conditions (https://onlinelibrary.wiley.com/terms-and-conditions) on Wiley Online Library for rules of use; OA articles are governed by the applicable Creative Commons License

Table 2. Some of the best performing commercially available POCT technology schematically evaluated against the most relevant REASSURED figures of merit.

		POCT Technology	LOD / LOI / LOQ	Diagnostic Sensitivity/Specificity	Time to Results [min.]	User Friendly?	Equipment Free?	Connectivity
Strip Tests	a	OraQuick Rapid HIV Test[70]	N.A.	99.8% / 100%	20–40	YES	YES	NO
	b	Chembio DPP HIV 1/2 Assay[71]	N.A.	98.9–99.9% / 99.9–100%	15–45	YES	YES	NO
	c	Clarity Strep A Test[72]	10^3 copies mL^{-1}[a)]	95% / 98.4%	<5	YES	YES	NO
Handheld	d	Cue Health[73]	N.A.	99.4% / 96.4%–99.4%	20	YES	NO	YES
	e	PEBBLE[74]	LOD = 10^3 copies mL^{-1}	94.28%–99.32% / 97.50%–100%	15–30	not too much	NO	YES
	f	LumiraDx[75]	LOD = 2 copies mL^{-1}	95.5% / 98.3%	<20	not too much	NO	YES
Portable	g	BinaxNOW Influenza Test[76]	10^3–10^4 copies $swab^{-1}$[a)]	93.5–99.7% / 94.2–99.8%	15	YES	YES	NO
	h	Abbot ID Now[77]	125 copies mL^{-1}[a)]	92.8–100% / 97.1–98.5%	13	not too much	NO	YES
	i	Q-POC[78]	LOD = 10 copies $reaction^{-1}$	99% / 100%	35	not too much	NO	YES
	l	Pluslife portable[79]	LOD = 400 copies mL^{-1}	96–98% / 96–100%	7–35	YES	YES	YES
		Pluslife Bench-top[79]					NO	
Small Footprint Bench-Top	m	SR-X SIMOA – Quanterix[80]	LOD = 1–10 × 10^{-18} M / 100 molecules mL^{-1}	N.A.	180–240	NO	NO	YES
	n	Cepheid GeneXpert[81]	38 IU mL^{-1} –131 CFU mL^{-1} – 250 copies mL^{-1}[a)]	84.3% / 100%	20–60	not too much	NO	YES
	o	Thermo ABI QuantStudio DX Real-Time PCR 4 470 660 – AV[82]	<100 molecule mL^{-1}[a)]	N.A.	30	NO	NO	YES

[a)] not specified if it is an LOD/LOI or LOQ.

from the background noise. Studies have proven that two species, for instance, an enzyme and its fluorescent substrate, will collide into each other in a timeframe of minutes generating a visible signal, when they are confined in a volume as small as 1 μm^3 or, equivalently, 1 femtoliter, fL.[32] But, top-notch optical systems are needed to actually measure the signal by the confined focal point of a visible laser beam to the diffraction limit, in a volume of ≈1 fL too. Consequently, a fluorogenic single molecule or one appropriately labeled one that enters this confined space can be identified utilizing fluorescence techniques with minimal background

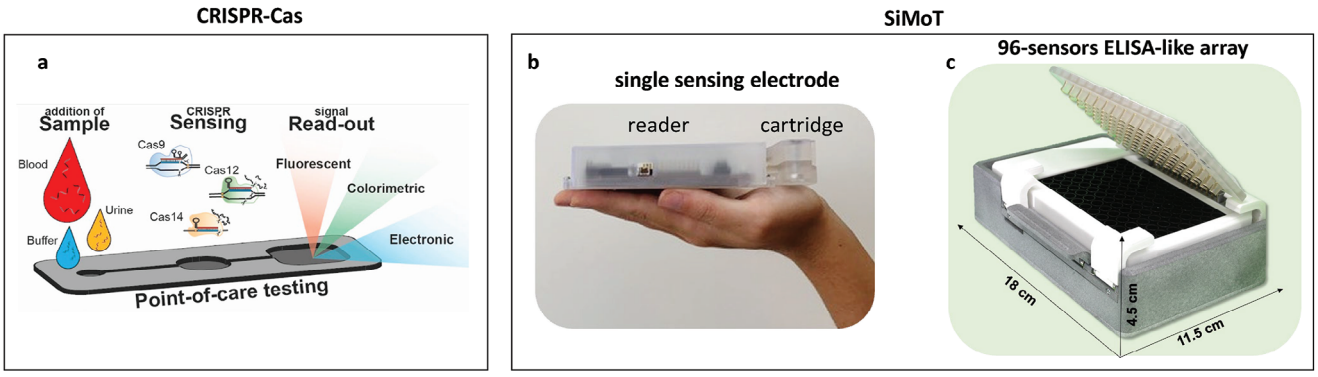

Figure 5. a) A general illustration on how the CRISPR/Cas9 technology is used for lateral flow strip tests POCT. Reproduced with permission from Ref. [95] Copyright 2020, Elsevier Ltd. b) A SiMoT handheld single sensor system targeting one marker at a time that is composed of a reader and a disposable accessory cartridge. Adapted and reproduced with permission from Ref. [13] Copyright 2022, AAAS under a Creative Commons Attribution-NonCommercial License 4.0 (CC BY-NC). c) SiMoT handheld multiplexing 96 sensors array. Adapted and reproduced with permission from Ref. [8] Copyright 2023, Wiley-VCH under Creative Commons Attribution 4.0 License (CC BY 4.0).

© 2023 The Authors. Advanced Materials published by Wiley-VCH GmbH

15214095, 0, Downloaded from https://onlinelibrary.wiley.com/doi/10.1002/adma.202309705 by Universita Di Brescia, Wiley Online Library on [22/01/2024]. See the Terms and Conditions (https://onlinelibrary.wiley.com/terms-and-conditions) on Wiley Online Library for rules of use; OA articles are governed by the applicable Creative Commons License

Table 3. The CRISPR/Cas and SiMoT against the REASSURED figures of merits.

POCT Technology	General Characteristics	Markers / Fluid assayed	Qualitative/ Quantitative	LOD / LOI / LOQ	Diagnostic Sensitivity/Specificity	Time to Results [min.]	User Friendly?	Connectivity	Affordability	Equipment Free	Del. to End-User
CRISPR/Cas	strip test; RPA[a], Cas9 [48]	M. pneumoniae-specific sgRNA in blood	quant.	3 copies[b]	100%/100%	30	YES	NO	YES	YES	NO
	strip test; LAMP[c], Cas 12[88]	SARS-CoV-2 – RNA in blood	qual.	LOD: 10 copies	N.A.	45	YES	NO	YES	YES	NO
	microarray; SG I as a fluorescent label, Cas9[89]	Methicillin-resistant Staphylococcus aureus_DNA in blood	N.A.	LOD: 10 CFU mL^{-1}	N.A.	N.A.	N.A.	NO	YES	YES	NO
SiMoT	single sensor_TRL[d] 5,6[13]	whole SARS-CoV-2 virus; Spike1, IgG in saliva	qual.	LOI: 1 protein in 0.1 mL	99.2% / 99.2%	21	YES	YES	YES	YES	YES
	96-sensor[8] array_TRL[d] 5,6	$KRAS^{mut}$ DNA and MUC1, CD55 proteins in blood for pancreatic cancer early diagnosis	qual.	LOI: 1 protein or 1 DNA copy in 0.1 mL	96% / 100%	90	YES	YES	depends on production scaling	YES	YES
	single sensor_TRL[d] 3,4	whole Xylella-fastidiosa bacterium directly in olive-sap[50] CRP,[90] Interleukin 6 (IL-6),[91] IgM,[92] IgG,[51] p24 protein of the HIV-1 virus capsid (p24-HIV-1),[93] and microRNA[94]	qual.	LOI: 1 bacterium in 0.1 mL	N.A.	N.A.	N.A.	NO	depends on production scaling	YES	YES

[a] RPA: Recombinase polymerase amplification;[136] [b] not specified if it is a LOD/LOI or LOQ; [c] LAMP: Loop-mediated isothermal amplification;[46] [d] TRL: Technology Readiness Level.[87]

© 2023 The Authors. Advanced Materials published by Wiley-VCH GmbH

15214095, 0, Downloaded from https://onlinelibrary.wiley.com/doi/10.1002/adma.202309705 by Universita Di Brescia, Wiley Online Library on [22/01/2024]. See the Terms and Conditions (https://onlinelibrary.wiley.com/terms-and-conditions) on Wiley Online Library for rules of use; OA articles are governed by the applicable Creative Commons License

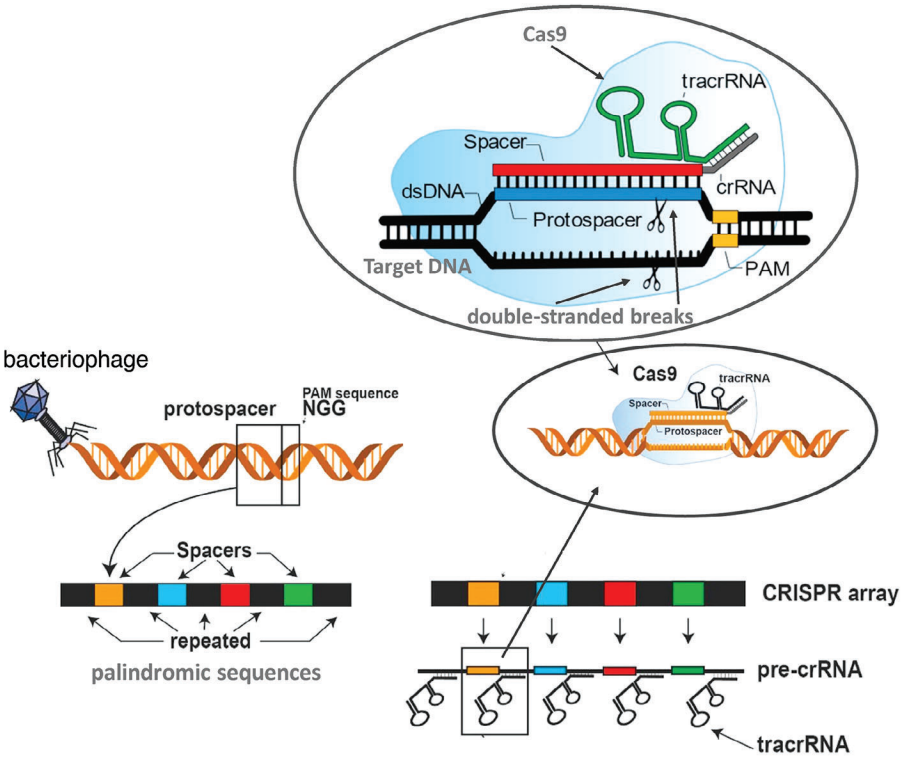

Figure 6. Scheme of the CRISPR/Cas9 principle, see text for details. Adapted and reproduced with permission of from Ref. [95] Copyright 2020, of Elsevier Ltd.

noise. However, as 0.1 mL 10^{11} fL can be found, one DNA for each fL is needed. But this occurrence is satisfied only when the target DNA concentration is at least in the nM range. To enhance the number of DNA copies from 1 to 10^{11}, techniques like PCR or loop-mediated isothermal Amplification (LAMP)[99] isothermal amplification are needed. LAMP, unlike traditional PCR, which requires cycling through different temperature stages, operates under constant temperature conditions making it well-suited for field applications, point-of-care diagnostics, and resource-limited settings. To visualize the detection, a label molecule is often used. The Cas conformational change upon binding, which triggers the activation of the label molecule that generates a detectable signal, such as fluorescence, color change, or luminescence, serves this scope. The activated label signal is then detected using appropriate equipment or devices. This can include fluorescence readers, colorimetric readers, or even smartphone-based cameras for point-of-care applications.[100]

CRISPR/Cas biosensing can be customized for various applications, such as diagnosing infectious diseases, detecting genetic mutations, identifying specific DNA sequences in environmental samples, and more. The technique's specificity and sensitivity make it a promising tool for rapid and accurate molecular diagnostics.

6.1.1. Principles

The CRISPR system serves as the foundation for adaptive immunity in bacteria and archaea. Its functioning principle is schematically shown in **Figure 6**. At its core, it employs Cas nucleases, enzymes, for example, a Cas9, with the ability to both bind to and generate double-stranded breaks within DNA molecules. When a bacterium gets infected by a virus, it employs a Cas nuclease to excise a segment of viral DNA called a protospacer. Specifically, a bacteriophage can integrate its genetic material into the bacterial cell, initiating a process of viral replication that eventually leads to the demise of the bacterial host. The protospacer segment is stored within the bacterial genome, alongside fragments from other viruses that have previously infiltrated the cell – generating a form of immune memory. These viral spacer fragments are interposed between repetitive palindromic sequences, thus giving rise to the name CRISPR.

Upon encountering the same virus during a subsequent infection, the bacterium can recognize and eliminate it using Cas9. Cas9 activity hinges on the presence of two RNA molecules: CRISPR RNA (crRNA) and trans-activating CRISPR RNA (tracrRNA). The crRNA corresponds to the viral spacer that was preserved following the initial infection, while the tracrRNA acts as a structural scaffold. The crRNA is complementary to the targeted DNA protospacer. These two RNAs collaborate to form a composite entity termed a guide RNA (gRNA). Cas9 can be visualized as a pair of scissors, with the gRNA functioning as the hand that guides the precise cutting. Prior to cutting the DNA, Cas9 functions as a searching tool, scrutinizing the viral DNA for a particular nucleotide pattern known as the protospacer adjacent motif (PAM), which is situated immediately following the target region. Once PAM, characterized by the NGG nucleotide sequence with "N" standing for any nucleotide base, is

© 2023 The Authors. Advanced Materials published by Wiley-VCH GmbH

15214095, 0, Downloaded from https://onlinelibrary.wiley.com/doi/10.1002/adma.202309705 by Universita Di Brescia, Wiley Online Library on [22/01/2024]. See the Terms and Conditions (https://onlinelibrary.wiley.com/terms-and-conditions) on Wiley Online Library for rules of use; OA articles are governed by the applicable Creative Commons License

recognized, Cas9 assesses the upstream area. If it identifies the target sequence indicated by the gRNA and the PAM, it induces a double-stranded break that disables the virus since viruses lack their own DNA repair mechanisms.

Jennifer Doudna and Emmanuel Charpentier co-discovered CRISPR. Their groundbreaking revelation came through the shed in 2012[36] when they showcased the CRISPR/Cas9 bacterial immune system's potential as a versatile gene editing tool. In 2020, Doudna and Charpentier were honored with the Nobel Prize in Chemistry for their pioneering contributions. Notably, this marked the first instance of the prize being awarded to a collaboration jointly led by two women. The CRISPR/Cas9 system discovery naturally led to the question: could Cas9, when directed by a different gRNA sequence, be employed to generate cuts at any desired genomic location? Their hypothesis was accurate, yielding revolutionary outcomes. The natural gRNA complex was transformed into a hybrid single guide RNA (sgRNA), presenting a straightforward and economical technique for genetic manipulation. Researchers simply needed to supply an alternate gRNA – which could be crafted relatively easily – and Cas9 could be utilized to generate incisions at various target sites within the DNA of any organism, provided the appropriate PAM sequence is present. CRISPR-diagnostic assays comprise two processes: a cis-cleavage reaction triggered by the target nucleic acid, activating the enzyme, and a trans-cleavage reaction in which activated enzymes non-selectively cleave single-stranded nucleic acids. In instances of extremely low target concentrations, the recognition and activation of the CRISPR enzyme (cis-cleavage) appear to be constrained by the diffusion of target molecules to the enzyme's active site.[101] To overcome the diffusion limitations, thermophoretic methods could offer a viable method to manipulate the analytical targets in homogeneous solutions.[102,103] Due to the temperature gradient, the target molecules are displaced toward the cooler region.

6.1.2. Amplification Effects

Among all amplification procedures, isothermal amplification methods require simple equipment and are unaffected by polymerase inhibitors, thus enhancing the robustness of the amplification process. Typically, they necessitate a processing duration of 15–60 mins. Among the most promising isothermal amplification methods well-suited for implementation within biosensing devices are LAMP, Nucleic acid Sequence-based Amplification (NASBA), Recombinase Polymerase Amplification (RPA), and Helicase-dependent Amplification (HDA).[104]

LAMP reaction exhibits the ability to identify very few[105] target nucleic acid sequences like RPA, as highlighted in Table 3, operating under isothermal conditions (typically ≈60–65 °C) facilitated by specifically crafted primer sets. LAMP reaction can be elucidated through three phases: an initial phase, a cycling amplification phase, and an elongation phase. To detect RNA viruses, an additional enzyme known as reverse transcriptase is required. This method is termed Reverse Transcriptase LAMP.[106] LAMP reaction involves the binding of specialized primers to target DNA or RNA. The primers include loop, inner, and outer primers, with a DNA polymerase that synthesizes new DNA strands while displacing the original ones. The amplification begins with the attachment of an outer primer to the target DNA, leading to the formation of a looped structure. Inner primers recognize these loops, initiating DNA synthesis and strand displacement. This creates a continuous loop of single-stranded DNA, serving as a template for exponential amplification. In each cycle, DNA synthesis and loop formation continue, resulting in a rapid increase in double-stranded DNA amplicons. LAMP is capable of swift amplification, generating a substantial quantity of DNA copies within approximately an hour, often surpassing conventional PCR by a factor of 100, all conducted within the temperature range of 60–65 °C.

NASBA is a highly resilient molecular technique engineered for the precise amplification of RNA sequences, demonstrating exceptional sensitivity and accuracy.[107] While traditional PCR primarily targets DNA amplification, NASBA is tailored for RNA-based targets, particularly advantageous for identifying RNA viruses and other RNA-related applications. The NASBA procedure starts with the binding of two primers to the target RNA sequence. These primers are specifically designed to match specific segments of the target RNA. The target RNA is transformed into complementary DNA through the catalytic activity of reverse transcriptase. This complementary DNA serves as the foundation for subsequent amplification steps. NASBA operates at a constant temperature, typically ≈41–50 °C, in contrast to the temperature cycling of PCR. RNA polymerase is utilized to produce multiple RNA strands from the complementary DNA template. These newly formed RNA strands replicate the original target RNA sequence. As RNA polymerase continues its synthesis of new RNA strands from the complementary DNA template, an amplification cascade unfolds, leading to an exponential increase in the quantity of the target RNA sequence. NASBA can achieve up to $\approx 10^9$-fold target amplification in 90 min.

RPA, as an isothermal amplification method, works effectively at relatively low temperatures.[108] This process accomplishes the amplification of the target sequence by employing recombinase enzymes, single-strand binding proteins, and a strand-displacement polymerase. Notably, RPA boasts the advantage of swift reaction kinetics without strict temperature control. RPA can detect even fewer than 10 copies, within a time frame of ≈20 min. RPA begins by having primers attach to their corresponding sequences on the target DNA or RNA. These primers are meticulously designed to match specific regions of the target sequence. Through the action of a recombinase enzyme, single-stranded DNA or RNA regions are displaced. This facilitates the formation of a primer-template complex, a critical step for amplification. A DNA polymerase enzyme extends the primers, synthesizing new DNA strands complementary to the target DNA or RNA template. This step leads to the creation of double-stranded DNA molecules. The DNA strands with primers now serve as templates for further replication.

HDA operates within a temperature range of 45–65 °C.[109] HDA employs a DNA helicase to initiate the separation of double-stranded DNA into single-stranded DNA. However, it is worth noting that the speed of amplifying lengthy target sequences is a constraint associated with this technique. HDA begins with the addition of a DNA template containing the target sequence. Specific primers are also introduced, which bind to complementary regions flanking the target sequence. In the HDA process, DNA helicase enzymes are introduced into the

© 2023 The Authors. Advanced Materials published by Wiley-VCH GmbH

15214095, 0, Downloaded from https://onlinelibrary.wiley.com/doi/10.1002/adma.202309705 by Universita Di Brescia, Wiley Online Library on [22/01/2024]. See the Terms and Conditions (https://onlinelibrary.wiley.com/terms-and-conditions) on Wiley Online Library for rules of use; OA articles are governed by the applicable Creative Commons License

Table 4. Advantages and disadvantages of isothermal amplification methods referred to CRISPR/Cas system-based biosensors.

Method	Advantages	Disadvantages
LAMP	-Single/few molecules sensitivity and high selectivity -Simplicity in primer design with multiple primers -Fast reaction at a constant temperature	The looped structure may increase the risk of nonspecific amplification
RPA	-Rapid amplification at low temperatures -Single/few molecules sensitivity and high selectivity	Susceptible to contamination due to its isothermal nature
NASBA	-Specifically designed for RNA amplification -Isothermal amplification of RNA at moderate temperatures -Single/few molecules sensitivity for RNA targets	Requires careful optimization for DNA targets
HDA	-Amplification at a constant low temperature. -Suitable for isothermal applications. -Not susceptible to matrix reactions in real samples	Limited commercial availability of HDA enzymes

reaction mixture. These enzymes play a crucial role in unwinding the double-stranded DNA template, leading to the formation of single-stranded segments. As the DNA transitions into a single-stranded state, the primers attach to their corresponding sequences on the DNA template. The DNA polymerase enzyme then extends these primers, creating fresh DNA strands that match the single-stranded template. These newly synthesized DNA strands act as templates for subsequent replication, leading to target DNA sequence exponential amplification. It's worth noting that in some cases, HDA may exhibit a slower amplification rate for longer target sequences when compared to certain other amplification methods.

When selecting an isothermal amplification method for CRISPR/Cas biosensors, factors such as sensitivity, specificity, reaction speed, temperature requirements, and ease of implementation should be considered. To this end, the main advantages and disadvantages of all isothermal amplification methods are summarized in **Table 4**.

6.1.3. CRISPR/Cas: Examples and Performance Level

CRISPR systems present a highly promising path for the accurate and sensitive detection of nucleic acids specific to pathogens. This capability has the potential to revolutionize a diverse array of on-site diagnostic and genotyping applications. One notable example is the application of CRISPR-based paper biosensing platforms, introducing an innovative approach that could significantly advance the field of pathogen detection and diagnosis.[37–47] In particular, the CRISPR/Cas9 system was employed to detect *Mycoplasma pneumoniae* (*M. pneumoniae*).[48] The newly developed biosensor leverages the potential of CRISPR/Cas9 for secondary recognition, a process that follows the preamplification of the target gene utilizing a dedicated set of primers. This strategic approach serves to mitigate the risk of false positives attributed to non-target factors. Leveraging the remarkable amplification efficiency and the capability of RPA to function at the relatively low temperature of 39 °C, extends the biosensor's LOD down to an amazingly low value of 3 DNA copies. **Figure** 7a,b report schematically the lateral flow biosensor developed by using the CRISPR/Cas9 system to detect *M. pneumoniae*, a bacterium that can cause respiratory tract infections in humans. The highly effective approach proposed allows for sensitive and specific detection of *M. pneumoniae* infections through a combination of RPA, CRISPR/Cas9 recognition, and visual analysis on a biosensor platform. The target gene selected for the detection is the P1 gene of *M. pneumoniae*, and a primer set (Biotin-FIP and BIP) is used during the RPA. This process generates multiple double-stranded DNA amplicons, termed ^{Biotin}dsDNA. These carry a biotin tag, a PAM, and a region for sgRNA binding. Following preamplification, the produced amplicons encounter the CRISPR/Cas9 system, featuring the Cas9 protein and a specific single-strand gRNA, which triggers the release of a short homologous sequence. This sequence binds to a gold nanoparticle (GNP)-probe, resulting in the formation of a complex named ^{Biotin}dsDNA-Cas9/sgRNA-GNP. The ^{Biotin}dsDNA-Cas9/sgRNA-GNP complex is introduced onto a lateral flow biosensor. Driven by capillary action, the mixture traverses the biosensor, passing through designated test (T) and control (C) lines. In the presence of *M. pneumoniae* infection, the biotin tag on the ^{Biotin}dsDNA-Cas9/sgRNA-GNP complex binds to pre-immobilized streptavidin on the T line. This leads to the accumulation of GNPs and visible red coloring. Conversely, when no *M. pneumoniae* is present, the ^{Biotin}dsDNA-Cas9/sgRNA-GNP complex does not form, and the T line remains non-colored. Regardless of the presence of *M. pneumoniae*, control probes on the C line captures any unbound GNP-probe. Hence, both C and T lines appear when the output is positive, whereas the presence of the sole C mark indicates a negative result. These optimal settings were employed to detect different concentrations of the *M. pneumoniae* DNA templates. The outcomes are illustrated in Figure 7c, where it's worth noting that the signal strength of the T line indicates a clear and direct correlation with the concentration of templates, falling within a range spanning from 3×10^0 to 3×10^6 copies. A plateau was observed in the T-line signal beyond 3×10^6 copies. This can be attributed to the depletion of primers in the preamplification system, rendering further amplification ineffective. Figure 7d reports the statistical analysis of the CRISPR/Cas9 lateral flow biosensor. Figure 7e reports the calibration of the CRISPR/Cas9 biosensor for *M. pneumoniae* detection. The coefficient of determination stands at 0.9837, and the LOD is established as 3 copies. Indeed, achieving such a remarkably low LOD is a significant accomplishment for a completely disposable and handheld system that can be operated by individuals without specialized training.

© 2023 The Authors. Advanced Materials published by Wiley-VCH GmbH

15214095, 0, Downloaded from https://onlinelibrary.wiley.com/doi/10.1002/adma.202309705 by Universita Di Brescia, Wiley Online Library on [22/01/2024]. See the Terms and Conditions (https://onlinelibrary.wiley.com/terms-and-conditions) on Wiley Online Library for rules of use; OA articles are governed by the applicable Creative Commons License

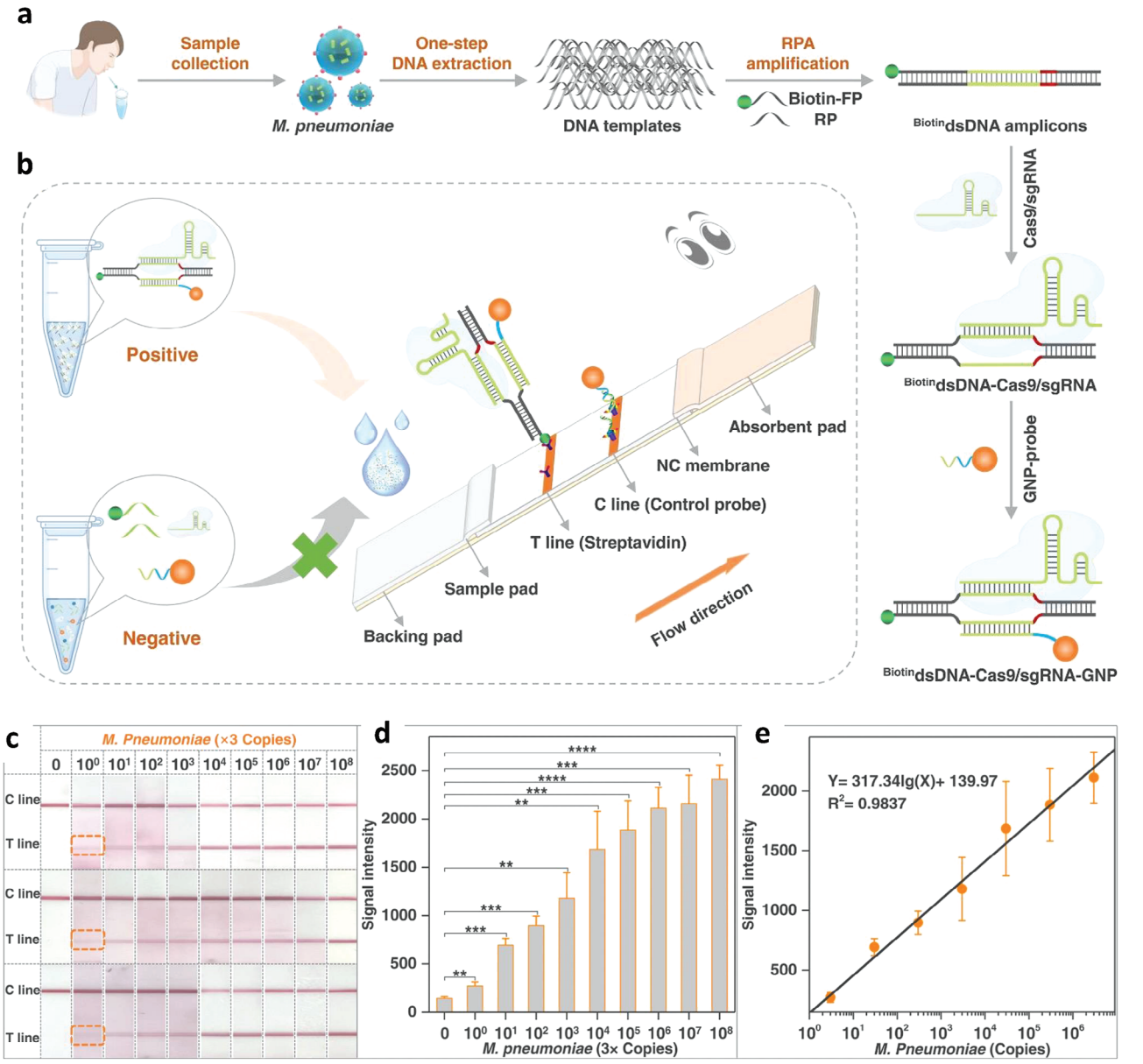

Figure 7. a) Scheme of the CRISPR/Cas9 biosensor to detect *M. pneumoniae*: sample collection, one-step DNA extraction, amplification by RPA, and target DNA recognized by CRISPR/Cas9; b) the CRISPR/Cas9 LFB to detect *M. pneumoniae*; c) the CRISPR/Cas9 lateral flow biosensor images at different of *M. pneumoniae* target copies; d) signal intensity analysis of CRISPR/Cas9 lateral flow biosensor T lines; e) calibration curve for CRISPR/Cas9 lateral flow biosensor. Adapted and reproduced with permission from Ref. [48] Copyright 2023, Elsevier Ltd.

Additionally, there have been reports of a CRISPR/Cas12 lateral flow biosensor assay designed for the detection of SARS-CoV-2 from respiratory swab RNA extracts, known as SARS-CoV-2 DNA Endonuclease-Targeted CRISPR Trans Reporter (DETECTR).[88] This platform combines the processes of reverse transcription and RT-LAMP technology. **Figure** 8a reports the schematic workflow of the DETECTR assay. The assay initiates with the extraction of RNA from nasopharyngeal or oropharyngeal swabs that have been preserved in the universal transport medium (UTM). Specifically designed primers are used to target the E (envelope) and N (nucleoprotein) genes of SARS-CoV-2, amplifying the regions employed by the World Health Organization assay (E gene region) and the US Centers for Disease Control and Prevention (US CDC) assay (N2 region within the N gene). However, these primers are adapted for the LAMP reaction. It's important to note that the assay deliberately excludes the targeting of N1 and N3 regions, as performed in the US CDC assay, due to the absence of suitable PAM sites within these regions. This lack of PAM sites makes them unsuitable for binding with the Cas12 sgRNA system. Particularly, the Cas12 single-strand guide RNA system is designed to detect several SARS-like coronavirus target sequences like in the assays involving multiple amplicons

© 2023 The Authors. Advanced Materials published by Wiley-VCH GmbH

15214095, 0, Downloaded from https://onlinelibrary.wiley.com/doi/10.1002/adma.202309705 by Universita Di Brescia, Wiley Online Library on [22/01/2024]. See the Terms and Conditions (https://onlinelibrary.wiley.com/terms-and-conditions) on Wiley Online Library for rules of use; OA articles are governed by the applicable Creative Commons License

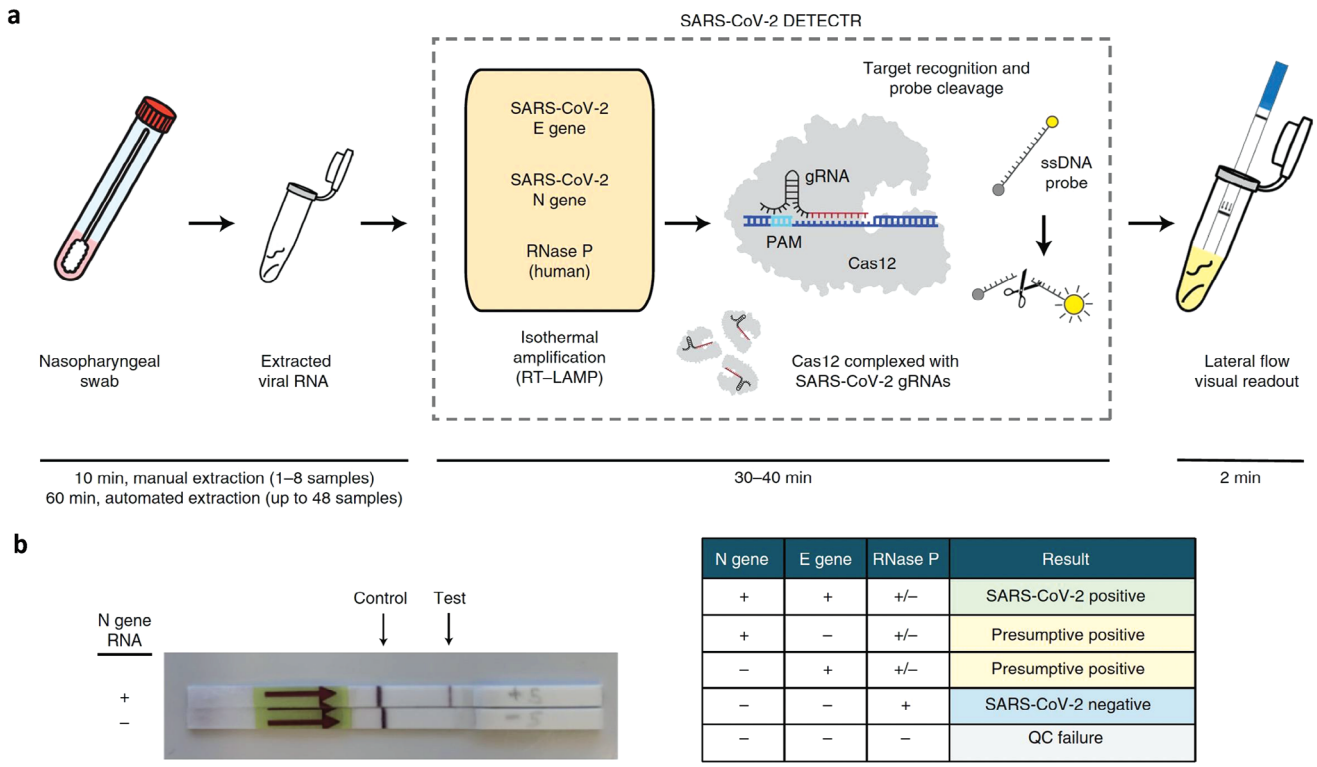

N gene	E gene	RNase P	Result
+	+	+/–	SARS-CoV-2 positive
+	–	+/–	Presumptive positive
–	+	+/–	Presumptive positive
–	–	+	SARS-CoV-2 negative
–	–	–	QC failure

Figure 8. a) Schematic representation SARS-CoV-2 DETECTR assay: nasopharyngeal swab, extraction of viral RNA, CRISPR/Cas12 recognition of amplified SARS-CoV-2 gRNA, and lateral flow visual readout; b) SARS-CoV-2 DETECTR assay run as a test and control toward N gene RNA and reading chart/diagnosis of SARS-CoV-2 DETECTR results. Adapted and reproduced with permission from Ref.[88], Copyright 2020, Springer Nature.

along with probes to either exclusively target SARS-CoV-2 or with the ability to recognize closely related SARS-like coronaviruses. Finally, the detection of the virus is confirmed through the cleavage of a reporter molecule.

The DETECTR lateral flow assay can be performed within a timeframe of 30–40 min (Figure 8b). A positive outcome is indicated by detecting both the E and N genes while detecting either the E or N gene gives a false positive result (Figure 8b). It's important to note that the visualization of the Cas12 scrutinizing reaction is achieved using a FAM-biotin reporter molecule. Additionally, specially designed lateral flow strips are employed to capture labeled nucleic acids.

In this process, reporter molecules that remain uncut are captured at the initial detection line, referred to as the C line. Conversely, if there is non-specific Cas12 cleavage activity, a signal is generated at the subsequent detection line, known as the T line (as depicted in Figure 8b). The DETECTR assay reported a LOD of 10 copies μL^{-1} reaction, which is higher compared to the CDC assay reporting 1 copy μL^{-1} reaction. However, the remarkable speed at which the development and validation of the SARS-CoV-2 DETECTR assay took place (less than two weeks for SARS-CoV-2) underscores the technology's potential to be rapidly deployed for diagnosing infections caused by emerging zoonotic viruses.

However, those molecular-based assays typically require sample pretreatment methods to extract the DNA/RNA to be analyzed. These methods generally encompass multistep processing of the patient's specimen involving sample heating in a range of 70–80 °C and lysis buffer. One of the primary hurdles in transitioning laboratory molecular assays into POC tests is the time and complexity involved in preparing samples from human and plant specimens. This process demands well-equipped laboratories and skilled personnel. To enable swift molecular diagnosis in settings with limited resources, there is a need for straightforward nucleic acid extraction techniques that do not rely on sophisticated instruments, thus enhancing field detection speed with minimal human involvement. Some novel POC sample preparation methods that exhibit significant promise for possible incorporation into compact nucleic acid amplification and detection platforms are now being proposed.[110]

Similarly, Koo and co-workers reported an enhanced molecular diagnostics tool incorporating a CRISPR/dCas9-mediated biosensor, which combines an inactivated Cas9 (dCas9) and a single microring resonator biosensor.[111] This innovative system enables the label-free and real-time detection of pathogenic DNA and RNA. The clinical applicability of this CRISPR/dCas9-mediated biosensor in tick-borne illnesses, such as scrub typhus and severe fever with thrombocytopenia syndrome, characterized by similar clinical presentations that pose challenges in differentiation has been investigated. Using the CRISPR/dCas9-mediated biosensor, the authors achieved single-molecule sensitivity for detecting ST (0.54 aM) and SFTS (0.63 aM). Notably, this detection sensitivity is 100 times greater than that of the RT-PCR assay. Moreover, the CRISPR/dCas9-mediated biosensor demonstrated the ability to clearly distinguish between scrub typhus and

© 2023 The Authors. Advanced Materials published by Wiley-VCH GmbH

15214095, 0, Downloaded from https://onlinelibrary.wiley.com/doi/10.1002/adma.202309705 by Universita Di Brescia, Wiley Online Library on [22/01/2024]. See the Terms and Conditions (https://onlinelibrary.wiley.com/terms-and-conditions) on Wiley Online Library for rules of use; OA articles are governed by the applicable Creative Commons License

severe fever with thrombocytopenia syndrome in serum samples within a rapid 20-minute timeframe. Based on the current literature, CRISPR/Cas systems-based biosensors will be widely employed as swift and accurate molecular diagnostic tools.[112]

6.2. SiMoT-Based Technology

6.2.1. The SiMoT Devices Architectures

The SiMoT "umbrella technology" comprises two platforms, both of which have reached TRL5-6. This means they have been validated in a relevant environment, and pre-clinical studies have been undertaken.[87] One platform comprises a single biofunctionalized electrode (single-sensor)[13] the other is a 96-wells ELISA-like array of biofunctionalized sensing electrodes.[8] The single sensor is designed for assaying a single marker/pathogen (e.g., the SARS-Cov2 virus), while the array can simultaneously assay multiple markers (multiplexing) and was used to assay the blood of pancreatic cancer patients. The latter is of critical importance as it equips clinicians with an advantage in the early diagnosis of progressive conditions like cancer.

The single-sensor assay platform is user-friendly and cost-effective, making it suitable for operation by untrained individuals, even at home or in resource-limited settings typical of underdeveloped countries. Conversely, the array technology is better suited for use by trained personnel, both in clinical settings and in decentralized facilities such as doctor's offices or small, partially equipped, clinical laboratories. In **Figure 9** a schematic representation of both devices is provided.

In Figure 9a,d pictures of the ultra-portable devices, both comprising reusable readers and a disposable accessory cartridge, of the single-sensor (Figure 9b) and of the array (Figure 9e,f), are shown. The two platforms are characterized by the following features:

- they operate via a capacitive coupling between a functionalized gate and a polarizing conducting system. In the single-sensor system, the coupling involves the extended gate of a FET (Figure 9c).[13] The Elisa-like array is based on a coupling between protruding functionalized 3D-sensing gates (Figure 9e) and the channel of an electrolyte-gated organic FET (EGOFET) printed on foil and glued at a bottomless standard 96-well ELISA plate (Figure 9f). A detailed structure of the SiMoT single EGOFET device fabricated in the well of an ELISA plate can be found in Ref. [113] In both cases, a shift in the electrochemical or surface potential of the sensing biofunctionalized gate due to the binding of a marker to the biological recognition elements, results in a threshold voltage (V_T) shift and a shift in the measured source-drain transistor current (I_D).
- The gates biofunctionalized with specific capturing antibodies or probes, are integrated into the disposable accessory cartridge, customized for the detection of a protein/antigen/pathogen analyte or of an oligonucleotide strand (DNA or RNA) that is specific for a given application. For the SiMoT platforms progressed to TRL5 the single-sensor cartridge was developed for the assay of the SARS-Cov2 virus directly in self-sampled saliva,[13] encompassing 240 samples. The 96-sensor array was employed to demonstrate the SiMoT platform capability for diagnosis of pancreatic cancer precursors when no symptom is yet apparent, proving the possibility of performing an assay directly in blood plasma in the framework of a pre-clinical trial involving 47 patients.[8] Moreover, many other assays have been performed so far involving a whole Xylella-fastidiosa bacterium directly in olive-sap[50] C-Reactive Protein (CRP),[90] Interleukin 6 (IL-6),[91] Immunoglobulin M (IgM),[92] IgG,[51] p24 protein of the HIV-1 virus capsid (p24-HIV-1),[93] and microRNA)[94] with a SiMoT device developed at TRL3-4 (prof-of-concept / technology validated in the lab) as listed in Table 3.
- In the disposable accessory cartridges, besides the biofunctionalized gate, a non-biofunctionalized gold gate, addressed as the reference gate, is also present to check at each stage of the sensing experiment, the stability of the signal in the cartridge and to make sure that any possible spurious fluctuation of the currents flowing in the transducing transistor channel is not ascribed to the sensing gate. In case the stability of the current flowing in the transducing transistors is not below 1–5% the cartridge is discarded.
- The electronic readout circuit readers are connected (Bluetooth or USB) to a smart device to enable direct data transfer to a smart device. For the array, a multiplexing flexible electronics and printed circuit board with a custom Si-IC chip (Figure 9g–i) are present to make the prototype form factor alike to that of a standard ELISA plate. The data acquired is managed through a dedicated app, and the AI-based analysis output categorizes the samples. All this makes SiMoT in principle particularly suited to implement the vision of a proactive and preventive healthcare system in the future, as portrayed in Figure 2.
- A sustainable version of the SiMoT invention is already under consideration. It's based on biodegradable and compostable materials from biomass and food waste along with additive printing techniques to minimize toxic processes. The printed bioelectronics is combined with a biodegradable 3D-printed fluidic cartridge and interfaced with a many-time-reusable, fully recyclable, battery-less Si-integrated circuit reader.

One other important aspect is SiMoT device scalability. The general applicability of the SiMoT platform combined with the testing for accuracy, reliability, and reproducibility demonstrated so far, are rather ideal conditions for scaling up the SiMoT platform from laboratory prototypes to mass production. Establishing efficient manufacturing processes is critical for cost-effective production. Bringing the SiMoT technology to the market is a multifaceted process. Key advantages of SiMoT include technology scalability with large-scale and low-cost manufacturing techniques, system integration, electronic processing, intelligent analysis, communication functionalities, and operating procedures compatible with the current standards in POC and ELISA diagnostic. Moreover, the SiMoT platform is a cutting-edge technology that has few competitors in the current in vitro diagnostic (IVD) market, offering a safe timeframe for entering the market and opening new market opportunities. On one side, this possibility is extremely relevant considering that the IVD market is rapidly evolving and highly competitive, with numerous established companies and products. On the other side, the scale-up of cutting-edge technology requires high-level technical experts. Indeed, industrializing SiMoT requires

© 2023 The Authors. Advanced Materials published by Wiley-VCH GmbH

15214095, 0, Downloaded from https://onlinelibrary.wiley.com/doi/10.1002/adma.202309705 by Universita Di Brescia, Wiley Online Library on [22/01/2024]. See the Terms and Conditions (https://onlinelibrary.wiley.com/terms-and-conditions) on Wiley Online Library for rules of use; OA articles are governed by the applicable Creative Commons License

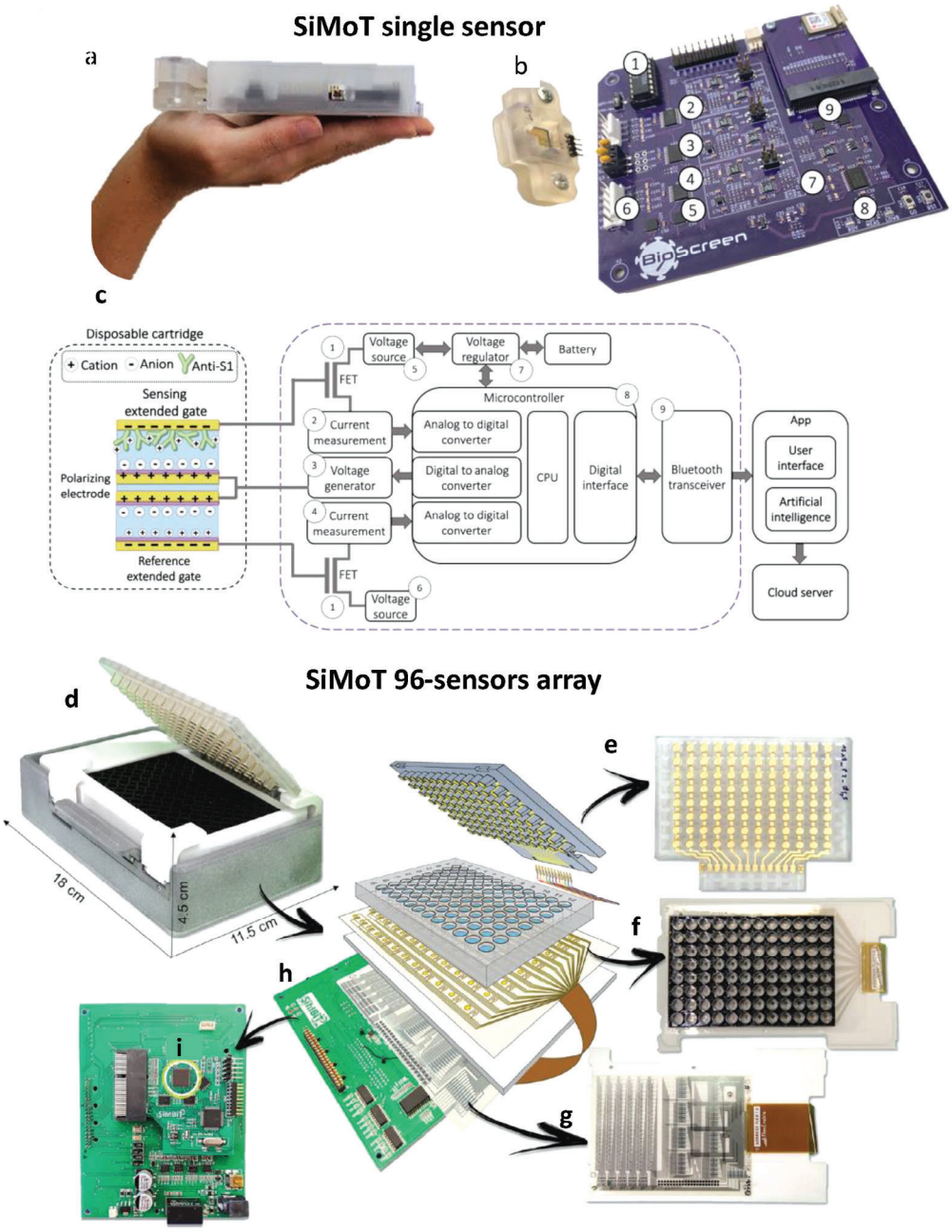

Figure 9. Upper panel – a) Picture of the handheld SiMoT single sensor bioelectronic device developed in the framework of the BioScreen project. b) Multi-time utilizable electronic driving and readout circuit to which a disposable cartridge is connected. c) Illustration of the functional principle of the cartridge (left) and description of all the components in the reader. Adapted and reproduced with permission from Ref. [13] Copyright 2022, AAAS under a Creative Commons Attribution-NonCommercial License 4.0 (CC BY-NC). Lower panel – d) Picture of the ultra-portable SiMoT ELISA-like 96-sensors bioelectronic array developer in the framework of the SiMBiT project; the device components are broken up in the center of the panel. e) The array of sensing 3D gates that are biofunctionalized with a given recognition element (capturing antibodies or oligonucleotides probes); the gates are pillars designed to protrude into the ELISA wells. f) The array of the EGOFETs is printed on foil and attached at the bottom of an ELISA plate that is purchased with no plastic bottom. g) Multiplexing electronics and printed circuit board encompassing a h) a custom Si-IC chip. Reproduced with permission from Ref. [8] Copyright 2023, Wiley-VCH under Creative Commons Attribution 4.0 License (CC BY 4.0).

© 2023 The Authors. Advanced Materials published by Wiley-VCH GmbH

15214095, 0, Downloaded from https://onlinelibrary.wiley.com/doi/10.1002/adma.202309705 by Universita Di Brescia, Wiley Online Library on [22/01/2024]. See the Terms and Conditions (https://onlinelibrary.wiley.com/terms-and-conditions) on Wiley Online Library for rules of use; OA articles are governed by the applicable Creative Commons License

15214095, 0, Downloaded from https://onlinelibrary.wiley.com/doi/10.1002/adma.202309705 by Universita Di Brescia, Wiley Online Library on [22/01/2024]. See the Terms and Conditions (https://onlinelibrary.wiley.com/terms-and-conditions) on Wiley Online Library for rules of use; OA articles are governed by the applicable Creative Commons License

expertise in various domains, including molecular biology, analytical chemistry, electronic engineering, material science, artificial intelligence, and biotechnologies. Finally, to bring the SiMoT technology to the market other relevant factors not strictly related to the technology should be considered, such as for example, the market demand and access, the regulatory requirements, the market adoption, and distribution.

The estimate of the costs for the SiMoT technologies is carried out by making, at this early stage, reasonable assumptions regarding several factors including the annual number of pieces produced and sold, product management expenses (such as after-sales service and product life cycle management), the cost of materials, assembly, and testing. Other product costs, such as IVD fees, representatives' fees, market expenses, etc., cannot be realistically calculated at this stage, and therefore, they are not accounted for in the provided estimation here provided. For the single-sensor technology assuming a highly conservative production and sales figure of 1000 units per year, the total cost is ≈160 euros reader^{-1} (with 50–60 euros allocated to materials/standard components). Conversely, for its disposable accessory cartridge, assuming a production of 100 000 units annually, the estimated total cost is ≈4 euros cartridge^{-1} (with 3 euros attributed to materials).

The bio-organic electronic reader of the multiplexing 96-array technology, produced at a very conservative rate of 100 units per year, results in a cost of ≈3000 euros reader^{-1} (with 300 euros associated with materials/components), while the accessory disposable cartridge for this technology, if produced at a rate of 10 000 units per year, incurs a total cost of ≈50 euros cartridge^{-1} (with 15–20 euros designated for the materials). This platform is to be used in a clinical setting and the reader is expected to be cheaper than bench-top instrumentation generally used in the clinics.

The scalability of the SiMoT technology will enable a further reduction in costs when scaling up production. For example, the single-marker technology reader, 10 000 pieces year^{-1}, develops a cost estimate of 65 euros reader^{-1} while for 1 000 000 cartridges year^{-1}, the estimated cost is 2.8 euros piece^{-1}. For the array platform, 1000 readers year^{-1} will cost 600 euros per reader while the 100 000 cartridges year^{-1}, will cost 18 euro per piece. Therefore, the costs of the SiMBiT analysis are expected to be competitive or even lower than those incurred for instance in the assessment of malignant pancreatic mucinous cysts diagnosis with standard cytopathological and NGS-based diagnosis.[8]

6.2.2. SiMoT Performance Level and Sensing Mechanism

SiMoT technologies are distinguished by a distinct set of attributes, detailed in the following:

- SiMoT can achieve a single-molecule limit of identifications in a 0.1 mL sample while ensuring a high level of reliability supported by diagnostic sensitivity and diagnostic selectivity exceeding 95–99%. To put this into perspective, it's worth noting that state-of-the-art technologies for the diagnosing of, for example, pancreatic cancer precursors typically achieve diagnostic sensitivities in the range of 60–70%.[8] The SiMoT technologies hold, hence, the potential to significantly reduce the occurrence of false negatives. Such an ability is of great importance for saving lives in less developed countries.
- the SiMoT devices, composed of a reusable reader and an accessory disposable cartridge specific for the early diagnosis of a disease, are ultra-portable and handheld. Moreover, they only require a smart device such as a tablet or a phone with a WI-FI connection to operate, which means that the devices function in a fully equipment-free environment.
- The SiMoT technology assays directly peripheral fluids such as blood or even saliva, making access to the sample simple and easy, including even the possibility of operating through self-sampling.
- Both proteins/antigens and nucleic acid strand markers can be assayed simultaneously from the same biofluid and with the same level of performance; this will open a completely new era in cancer and disease early diagnosis.
- Nucleic acid strand markers can be assayed with no need to be coupled with any amplification reaction; this simplifies the sample preparation to a minimum.
- The assays are rapid, with results obtainable in ≈20 min for the single marker and about an hour for the array, and the single sensor one is also user-friendly. Videos of the assay procedures can be found in the supporting information of Refs. [8,13]
- SiMoT technologies can address – by just changing the recognition element, for example, the capturing antibody (to target a specific antigen/protein) or the probe (to bind a specific oligonucleotide) integrated with the disposable accessory cartridge – many different diseases.
- The electronic reader and data collection enables straightforward and convenient remote control of the entire assay process. In fact, the final deliverable to end-users is straightforward and direct. Full data connectivity facilitates integration with digital platforms and seamless connectivity to electronic health records, streamlining data management, analysis, and reporting.

Collectively, these qualities render the SiMoT technologies uniquely well-suited for POCT screenings among asymptomatic individuals allowing for the highly reliable, rapid, and cost-effective identification of those who are ill. As can be appreciated by looking at Table 2 and Table 3, the relevance of SiMoT. The advantage over the CRISPR-based technology, combined with enzymatic amplification, is that SiMoT enables POCT detections, with the same level of performance of both proteins and oligonucleotides.

The reason why SiMoT can achieve such a high level of performance can be attributed to the combination of three highly important specific features:

- the amplification effect propagates the electrostatic shift upon binding, which is associated with the conformational change in the single antigen/probe binding event. This effect extends to a much larger number of recognition elements, ultimately altering the surface electrostatic potential over a significantly larger area of the biofunctionalized electrode surface.
- The operation of the SiMoT device as a qualitative YES–NO Boolean assay.
- The use of Artificial Intelligence algorithms to automatically sort out the YES–NO samples.

© 2023 The Authors. Advanced Materials published by Wiley-VCH GmbH

In the following these three key aspects are reviewed in detail.

Amplification Effect in SiMoT: The remarkable LODs and LOIs achieved by SiMoT arise from surface potential (*SP*) electrostatic variations due to the occurrence of antigen–antibody binding events on a millimeter-wide gate surface that have been densely functionalized with capturing antibodies. These occurrences result in a change in the threshold voltage (ΔV_T), which, in turn, modifies the conductance of the transistor channel, generating a noticeable response associated with the SP shift, surpassing the background noise level. The SiMoT platform's exceptional ability to detect single proteins, even when the detecting surface is covered by a sparsely attached antibody film, suggests the presence of amplification effects that transmit changes in surface dipole distribution.

To elaborate further, the study demonstrates that a few antigen-antibody interactions lead to a significant surface potential shift across a large-area bio-functionalized gold surface. This has been verified by means of an atomic force microscopy and Kelvin probe force microscopy (KPFM) study.[114] **Figure 10** exhibits KPFM images in the central panels while, in the right panels histograms representing surface potential differences (SPD) of a gold electrode are suitably patterned with an anti-IgM layer. The analyses are systematically performed before and after a few individual binding events have occurred. Notably, we establish that although SP values in specific areas may vary due to external factors, the average relative contact potential difference between the bio-functionalized and Au areas, denoted as $SPD \equiv SP_{biolayer} - SP_{Au}$ remains virtually unaffected by artifacts and exhibits an exceptional sensitivity to surface alterations brought about by affinity-binding events.

The left panels (Figure 10a,d,g,l) offer a schematic representation of each experiment performed in the measurement protocol. The top row displays the outcomes associated with the as-prepared gold sample covered with the anti-IgM layer. The subsequent rows depict the gold/anti-IgM sample exposed to Immunoglobulins G (IgGs) that does not bind to anti-IgM and bind IgMs, respectively. The saline solutions of antigens in phosphate buffer (PBS) are used to simulate physiological conditions. Specifically, Figure 10b,c shows KPFM images and the average SPD value (176 ± 20 mV) for the pristine gold/anti-IgM interface, serving as a baseline. Figure 10e,f exhibits KPFM images and an SPD value of 167 ± 20 mV, obtained after incubating the sample in a 3 fM IgG solution for 10 min, which functions as a negative control. Following that, the gold electrode covered with anti-IgM is exposed to the IgM binding solutions. Remarkably, after incubation in PBS solutions containing 100 zM and 10 aM IgM, the KPFM images change significantly, as shown by Figure 10h,m. Also, Figure 13i,n, shows a decrease by $\Delta SPD = -48 \pm 20$ mV and $\Delta SPD = 60 \pm 20$ mV, in comparison with the initial baseline. Importantly, The KPFM images validate that this significant shift occurs uniformly across the entire 90 µm × 90 µm region encompassing ≈6 million anti-IgM capturing proteins. This is notable considering the relatively low number of antigens (≈1000 IgM) found within the 0.1 mL incubation volume. They are molecules capable of diffusing and meeting the extensive surface area occupied by the anti-IgMs. These results offer concrete experimental proof that even a limited number of antigen–antibody binding events can trigger substantial alterations in surface potential across extensive biofunctionalized Au surfaces. This suggests that electrostatic interactions between closely arranged capturing antibodies on the gate surface can propagate an electrostatic change originating from a single capturing antibody, in a domino-like mode. This phenomenon is highly significant and offers insights into the electrostatic behavior of antibody films attached to electrode surfaces.

Qualitative YES–NO Boolean Assay: A SiMoT device operating as a YES–NO qualitative assay is meant to be able to correctly classify a positive (YES) or a negative (NO) sample when in a 0.1 mL sample there is, or there is not at least one marker. The threshold that is used is the LOD or LOI level which assures higher reliability. **Figure 11** illustrates how this is performed for the case of a negative/NO patient (Figure 11a) and the case of a positive/YES (Figure 11b). After bio-functionalizing the sensing gate electrode may be just by the physisorption of a layer of capturing antibodies,[49] this sensing electrode is incubated into a reference fluid for ten minutes. The reference fluid is specific for a given biofluid and its choice is a critical part of the optimization of a given assay. As an instance, for assays in saliva, the 1,4-piperazinediethanesulfonic acid (PIPES) buffer solution (pH 6.8, 0.5 M) was used, while for the swab the UTM from Copan served for this scope.[13] For blood plasma[8] and olive sup[50] the PBS solution (pH 7.4, 163 mM) worked very well.

A given sensing-gate gate is washed, after incubation the reference fluid, in deionized water and measured in deionized water where the capacitive coupling occurs.[115] Here a set of 10–15 source-drain currents (I_D) versus gate bias (V_G) at fixed drain bias V_D (transfer characteristics), are measured and this is addressed at the "gate cycling".[13] The point values at a given V_G (usually at the maximum of the transconductance) versus cycling time are plotted as shown on the left part in Figure 11a,b. Here the stabilization dynamic curve of the gate can be used as the baseline trace. Afterward, the very same gate is incubated for 10 min in the sample to be assayed, it is then washed and measured following the same protocol used for the measurement of the baseline. The data in Figure 11a show that for the NO sample the stabilization dynamic curve measured in a healthy patient is very much alike to that measured in the reference solution.

The protocol foresees that many replicates (≈7–10) of negative samples (or of negative control experiments) are measured with the same gate (or with different nominally identical gates), to measure the average transient curve and the standard deviation for a given assay. For the sake of clearness, the dispersion of the noise is not given in Figure 11. With these data, the Gaussian distribution of the noise for this assay can be plotted and the curve can be seen in the rightmost part of Figure 11. Once the Gaussian distribution function of the assay noise is plotted, the same Gaussian distribution for the level of the LOI can be depicted as well as explained in Section 4. The same protocol is used to measure a positive-YES sample and the stabilization dynamic curve is shown on the right of Figure 11b. As it is apparent the curve this time is completely different from the baseline and very relevantly, goes well below the LOI level.

To automatically discriminate the YES and NO samples, these data can be characterized by a set of numerical parameters that are relevant to features that are analyzed by an AI approach.

The Role of Artificial Intelligence in SiMoT Assays: POCT assays typically provide qualitative diagnostic answers, sorting between positive (YES) and negative (NO) samples. Those tests

© 2023 The Authors. Advanced Materials published by Wiley-VCH GmbH

15214095, 0, Downloaded from https://onlinelibrary.wiley.com/doi/10.1002/adma.202309705 by Universita Di Brescia, Wiley Online Library on [22/01/2024]. See the Terms and Conditions (https://onlinelibrary.wiley.com/terms-and-conditions) on Wiley Online Library for rules of use; OA articles are governed by the applicable Creative Commons License

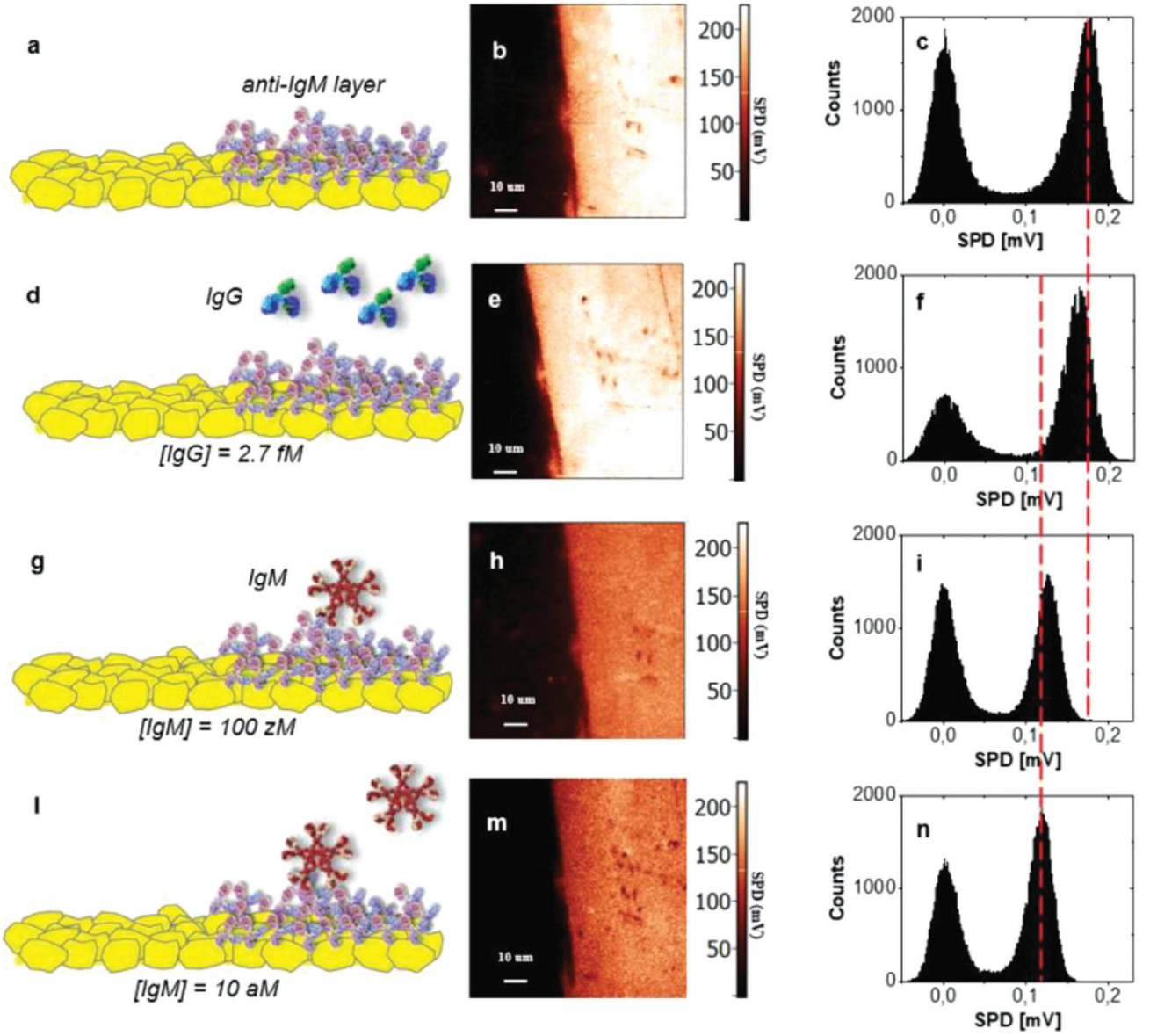

Figure 10. Surface potential alterations resulting from binding events driven by molecular affinity. a) schematic cross-sectional view. b) KPFM image covering a 90 μm × 90 μm region, situated proximate to the junction between the untreated gold (on the left) and the gold surfaces functionalized with anti-IgM antibodies (on the right). The physically adsorbed anti-IgMs act as the initial layer for capturing. In panel c, a histogram is provided illustrating surface potential values. These values are plotted based on the SPD between the local and the highest observed SPD values on the untreated gold surface. Additional sets of panels {d, e, f}, {g, h, i}, and {l, m, n} follow the same format as {a, b, c}. These panels present cross-sectional perspectives, KPFM images, and SPD histograms for a sample that underwent consecutive exposures to a phosphate buffer saline solution (pH = 7.4, ionic strength = 163 mM). Specifically, panel d shows the results when the sample was exposed to IgG (not binding to anti-IgM) at a concentration of 3 fM (serving as a negative control), panel g depicts the outcome of exposure to IgM at 100 zM, and panel l illustrate the results of exposure to IgM at 10 aM. Adapted and reproduced with permission from Ref. [114] Copyright 2022, Wiley-VCH under Creative Commons Attribution 4.0 License (CC BY 4.0).

are used to determine the presence or absence of a particular biomarker in the assayed peripheral body fluid. In light of the complex nature of matrix solutions such as serum, blood, urine, and saliva, coupled with the common practice of analytical assays yielding multiple measurements for each sample being examined, the utilization of multivariate data processing techniques proves to be exceptionally advantageous.[116] Indeed, the validation of POCT technologies still relies on the analysis of a single variable/feature that varies based on the concentration of the target biomarker, that is, involving univariate analysis. Nonetheless, the task of singling out a primary variable/feature to describe a phenomenon can be intricate and subjective, potentially resulting in data reduction when handling extensive datasets. Therefore, efforts have been directed toward developing machine-learning approaches for characterizing patients' samples to identify a specific biomarker.[117,118]

© 2023 The Authors. Advanced Materials published by Wiley-VCH GmbH

15214095, 0, Downloaded from https://onlinelibrary.wiley.com/doi/10.1002/adma.202309705 by Universita Di Brescia, Wiley Online Library on [22/01/2024]. See the Terms and Conditions (https://onlinelibrary.wiley.com/terms-and-conditions) on Wiley Online Library for rules of use; OA articles are governed by the applicable Creative Commons License

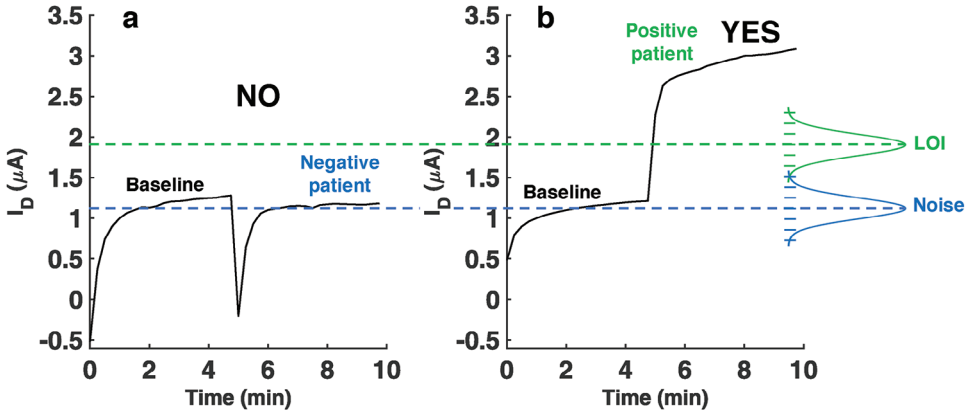

Figure 11. Schematic representation of the YES–NO Boolean SiMoT assay. The stabilization dynamic curves (see text for details) for the case of negative healthy patients are shown in panel (a) while the same curves for the case of a positive ill patient output are given in panel (b).

In this scenario, principal component analysis (PCA) stands out as a widely favored multivariate method. It enables the generation of a suitable number of principal components while minimizing information loss.[119] PCA is an unsupervised statistical technique primarily employed for exploratory multivariate data analysis, detecting outliers, and visually revealing clustering patterns. PCA, by using a statistical process that utilizes orthogonal transformations, transforms a dataset containing potentially correlated variables into a fresh set of linearly uncorrelated variables, commonly referred to as principal components. Those new variables are a standardized linear combination of the original variables, featuring both positive and negative contributions, facilitating a comprehensive understanding of complex multivariate phenomena. Additionally, PCA provides the capability to decrease system dimensionality through the identification of more representative linear combinations of the initial variables. Recently, PCA has been undertaken to analyze the whole SiMoT 96-sensors array' data set, to investigate the presence of graphical clustering among the blood plasma and pancreatic cyst fluids belonging to high-grade, low-grade mucinous cyst, and control groups.[8] The PCA analysis revealed distinct graphical clustering among the high-grade samples, whereas the low-grade and control group samples exhibited significant overlap. Furthermore, this approach enabled the investigation of correlations among various biomarkers in relation to the progression of mucinous lesions. The analysis highlighted a higher content of the MUC1 oncoprotein in low-grade mucinous samples, while high-grade mucinous samples were characterized by the onset of the CD55 oncoprotein.

While PCA serves as a simple yet potent method for extracting insights from complex systems, it is not well-suited for predictive modeling. To address this limitation, specialized multivariate supervised methods have been devised for sensors and biosensors.[120] In the pursuit of this goal, classification algorithms are widely recognized as supervised techniques designed to predict categorical outputs, involving a finite set of class labels. These algorithms can handle classification tasks ranging from binary to more complex multi-class scenarios. These techniques establish mathematical principles or models capable of describing a sample based on a qualitative attribute, like its affiliation with a particular category. To fulfill these criteria, two classes of multivariate pattern recognition methods are utilized: discriminant classification and class modeling.[121] The method addressed as discriminant, classifies specimens into one of several pre-established categories, typically comprising a minimum of two categories. Conversely, class modeling, also known as one-class classification,[122] assesses if the assayed biofluid aligns with the characteristics of a specific target class or not. This fundamental distinction holds considerable practical importance. For example, when adopting the discriminant approach, it is crucial to have fully representative sampling for all the categories, a demand that can be quite challenging in numerous clinical scenarios. In contrast, class modeling approaches necessitate just a sole sample representative of the targeted category to construct verification models that are unbiased. Methods addressed as one-class classification, therefore, prove highly advantageous in various clinical applications.[123,124] However, their utilization of POCT technologies remains somewhat limited. On the other hand, discriminant methods are the most used in biosensing applications. Among others the k-nearest neighbors,[8] partial least squares discriminant analysis,[125] linear discriminant analysis,[126] and quadratic discriminant analysis can be mentioned.[127]

Recently, a discriminant analysis to sort COVID-19 negative and positive samples of patients' saliva was developed based on a multilayer perceptron network (MLPn).[13] This algorithm operates on the basis of perceptron (neuron) nodes organized in layers, linked to preceding and subsequent layers following a predefined pattern. Every perceptron forms a linear combination of input values and produces an output by traversing a sigmoid function, like the logistic function in binary classification, which scales the result to fall within the 0 to 1 range. The multi-layer perceptron approach receives input from the R sensing response, representing the relative current change upon exposure to the saliva sample, and R_D, addressing dynamic processes occurring at the gate electrode associated with the setting of the capacitive coupling between the electrode and electrolyte. These feature values were derived from each of the 240 raw data points.

In **Figure 12a**, the distribution of the samples sorted as negative and positive ones, is visualized in a 2D feature space (negative ones are in blue while positives are in red). Figure 12b

© 2023 The Authors. Advanced Materials published by Wiley-VCH GmbH

15214095, 0, Downloaded from https://onlinelibrary.wiley.com/doi/10.1002/adma.202309705 by Universita Di Brescia, Wiley Online Library on [22/01/2024]. See the Terms and Conditions (https://onlinelibrary.wiley.com/terms-and-conditions) on Wiley Online Library for rules of use; OA articles are governed by the applicable Creative Commons License

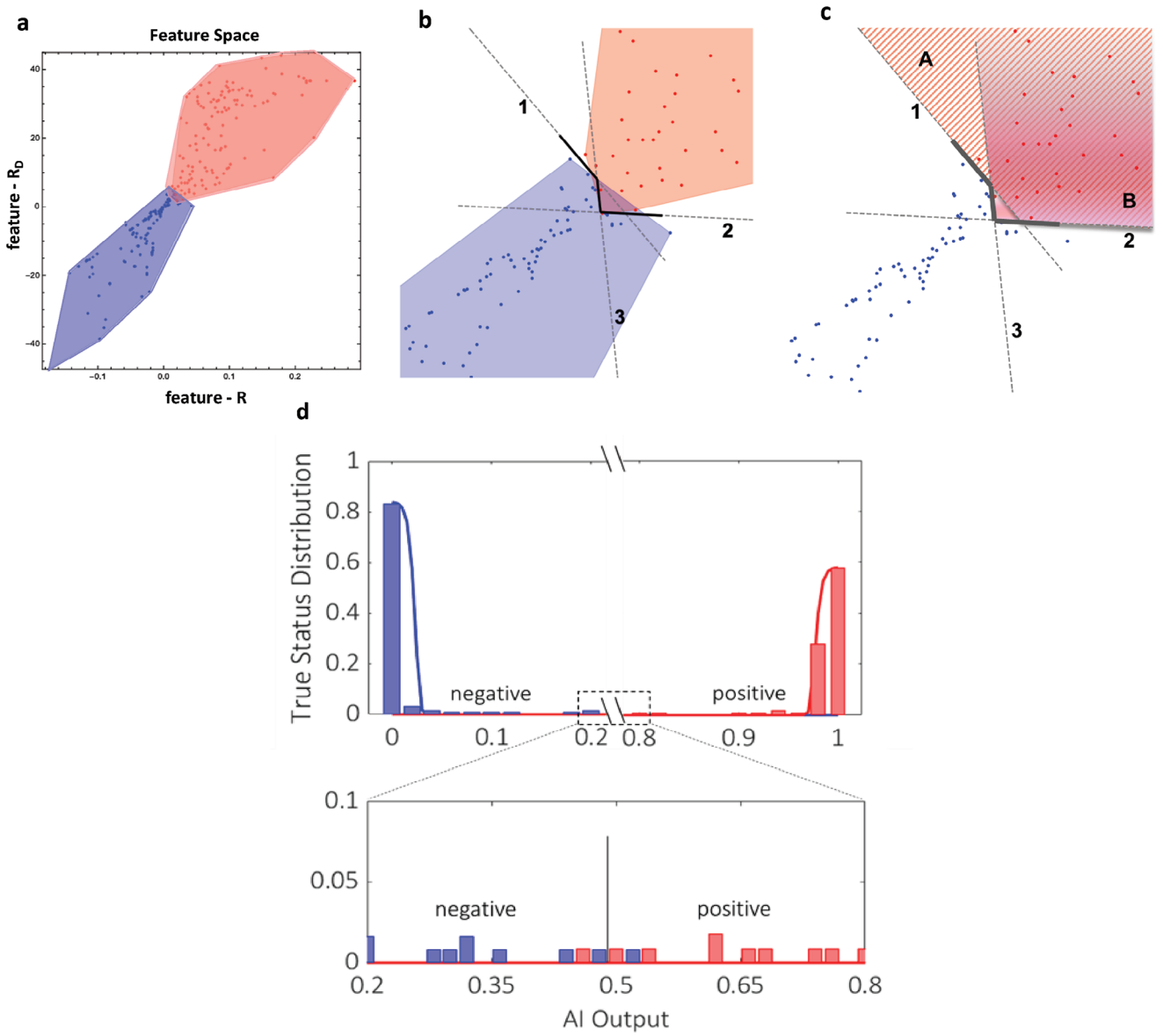

Figure 12. Schematic representation of the 2D Feature Space for the *R* and R_D values. a) All the SiMoT 240 samples assayed in the 2D Feature Space. The negative samples are given in blue while the positive ones are given in red. b) Zoom into the central region of the plot; black lines 1, 2, and 3 are the boundaries defined by the first layer perceptrons of the binary classifier. c) The convex regions A and B are defined by the perceptrons. d) Histograms displaying the actual sample status (negative or positive) in comparison to the SiMoT discriminant classifier output for all 240 assayed samples from Ref. [13] Copyright 2022, AAAS under a Creative Commons Attribution-NonCommercial License 4.0 (CC BY-NC).

demonstrates that the MLPn establishes a boundary function dividing the 2D feature space into two parts. Specifically, the merging of regions A and B in Figure 12c forms a concave area encompassing all positive specimens (P), with just one false negative and one false positive errors out of 240 assays. Notably, outside the combined A and B regions all the negative specimens (N) are correctly classified. In Figure 12d, the plot illustrates the distribution of sample classes relative to the output of the discriminant classifier for the complete SiMoT dataset. Blue bars represent negative cases, while red bars represent positive cases. Solid lines are utilized to illustrate Gaussian distributions for both negative and positive samples, where the mean values are set to 0 for negatives and 1 for positives. The graph visually presents clearly distinguishable output data for these two sets. Upon closer scrutiny of the central region, where potential errors may arise, one can observe a solitary red point within the blue region and a lone blue point within the red region. These isolated instances correspond to one false negative among 121 negative results in the blue region of the plot and a single false positive amidst 119 positive outputs in the red region. Consequently, the overall error rate stands at 0.83%, corresponding to one misclassification of a negative sample and one misclassification of a positive sample.

© 2023 The Authors. Advanced Materials published by Wiley-VCH GmbH

15214095, 0, Downloaded from https://onlinelibrary.wiley.com/doi/10.1002/adma.202309705 by Universita Di Brescia, Wiley Online Library on [22/01/2024]. See the Terms and Conditions (https://onlinelibrary.wiley.com/terms-and-conditions) on Wiley Online Library for rules of use; OA articles are governed by the applicable Creative Commons License

6.2.3. SiMoT: Examples and Performance Level

In **Figure 13** the actual data for the SARS-CoV-2 virus detection with the SiMoT single-sensor directly in saliva as well as of the Spike1 (S1) protein both in saliva and blood detection are shown in the upper panel (Figure 13a–c). In the lower panel, the data measured with the SiMoT array to detect the MUC1 protein marker for the early diagnosis of mucinous cysts precursors of pancreatic cancer, are shown (Figure 13d–l).

More in detail in Figure 13a the detection of the SARS-CoV-2 in patients' saliva (43 ± 7 viruses in 0.1 mL) by means of a gate-sensing electrode bio-functionalized with the anti-Spike1 capturing antibodies, is proposed. The central panel features the stabilization dynamic curves, according to what is already described in Figure 11, composed of a part measured in the PIPES reference fluid and another in saliva. The blue curve is relevant to a negative patient, while the red one is relevant to a positive one. The rightmost panel is the output of the binary classifier described in the previous section. In Figure 13b,c the same data are presented for the detection of the S1 protein, at an anti-S1 functionalized electrode, in saliva (160 zM or equivalently 10 ± 3 S1 in 0.1 mL) and blood (30 aM – 1.8×10^3 S1 in 0.1 mL) respectively. In the latter case, the reference fluid is PBS. The whole study involved the assay of 240 samples with just one false negative and one false positive, resulting in diagnostic sensitivity and specificity as high as 99.2%.[13]

In the lower panel of Figure 13, the SiMoT assay of the Mucinous1 (MUC1) proteins performed with the SiMoT array, is shown. This is, along with CD55 (protein) and KRAS (mutate oligonucleotide strand), one of the three markers that were used in the early detection and sorting of pancreatic cysts that can be precursors of pancreatic cancer. The detections involved a cohort of 47 patients and the markers were assayed both in the very accessible patients' blood plasma and in the cyst fluids that were collected with endosonography.

More in detail in Figure 13d,e the data relevant to the negative control experiment are shown. In this case, the sensing gate was biofunctionalized with bovine serum albumin (BSA) that does not bind specifically to other biological species but only to anti-BSA. The BSA sensing-gate is incubated et first in PBS (reference fluid) and afterward in PBS added with KRAS, MUC1, and CD55 at 10 nM. In Figure 13d the transfer characteristics (I_D versus V_G) measured sequentially during the cycling of the electrode in PBS (blue curves) and in PBS added with KRAS, MUC1, and CD55 (red curves), are shown. As it is evident (also from the inset showing a magnified portion of the curves) they all overlap, meaning that no appreciable change of the gate surface potential is detected. This implies that no binding occurred, proving that indeed this setting of curves serves as an excellent negative control experiment. In Figure 13e the same data are plotted (as a red curve) at a fixed V_G and the current data points from altogether, the dynamic curves plot measured during the cycling time. More precisely, the red curve is the average trace over 7 replicates, measured simultaneously, on different BSA functionalized sensing-gates in the SiMoT array; the area shaded in light gray is the standard deviation. The gray curve in the bottom-right of Figure 13e is the resulting random error Gaussian distribution. The LOI level is eventually set by shifting the Gaussian error distribution by 6 standard deviations. The black dotted curve is the shift of the current measured with the bare gold reference electrode showing the very high stability of the system during the sensing.

These data set the stage for the actual assay performed with a sensing-gate biofunctionalized with the anti-MUC1 specific capturing antibody, whose results are given in Figure 13f,g. In the former figure the transfer characteristics measured during the cycling in PBS (blue curves) and in PBS added with the sole MUC1 at a concentration of 10 zM, which means 1 ± 1 MUC1 protein in 0.1 mL of PBS (red curves), are shown. Despite the single-molecule presence of MUC1, a shift of the red transfer curves compared to the bleu ones is clear. This is also evident in Figure 13g, where the LOI level is set based on the negative control experiment and the red line is the sensing on the anti-MUC1 electrode; indeed, the red trace in the presence of only one binding protein goes well beyond the LOI level proving that the sample does contain at least one molecule of MUC1. In this figure, the black dotted curve is the shift of the current measured with the bare gold reference electrode.

In Figure 13h,i,l, the same protocol is engaged to measure blood (Figure 13h,i) and cyst fluid (Figure 13l) samples from patients who were independently diagnosed to have a high-grade mucinous cyst (high-probability to develop a pancreatic cancer), a potentially low-grade mucinous cyst (low-probability to develop a pancreatic cancer), or a non-mucinous cyst (benign cyst). The data clearly show that in the high-grade case, a very large signal is measured that goes well beyond the LOI (Figure 13h), while a signal below the LOI is measured for the potentially non-mucinous (Figure 13l), and a signal just slightly higher than the LOI is measured in the low-grade lesion (Figure 13i). Similar data were gathered for CD55 and KRAS.[8]

During the study, a combination of proteins (MUC1, CD55) and a mutated oligonucleotide strand (KRAS) were identified in blood plasma and cyst-fluid of 47 patients. This discovery aimed to distinguish mucinous cysts and categorize those with high-grade characteristics, which are considered precursors to cancer in the pancreas organ. Following the simultaneous assay of these specific biomarkers, a machine-learning-based classifier successfully identified a subgroup of ten samples assayed in a double-blinded way. Notably, when considering all three markers comprehensively, the results show a diagnostic sensitivity of 96% and a diagnostic specificity of 100% in detecting mucinous neoplasms and identifying those with high-grade features, both in cyst fluids and blood plasma. Additionally, the SiMoT technology proved to be quicker and cheaper than current diagnostic procedures. It is solely the assay capable of simultaneously testing genomic and protein markers both at the single-molecule level.

7. Critical Evaluation of Approaches Encompassing the Screening of Asymptomatic Individuals

The vision of reaching the early diagnosis of diseases through the screening of a population is seen as a perspective that has the potential to generate benefits for citizens. Effectiveness in diagnosing infectious diseases relies on adherence to crucial standards such as affordability, accessibility, and accuracy in diagnostic tests. The World Health Organization, as already discussed,

© 2023 The Authors. Advanced Materials published by Wiley-VCH GmbH

15214095, 0, Downloaded from https://onlinelibrary.wiley.com/doi/10.1002/adma.202309705 by Universita Di Brescia, Wiley Online Library on [22/01/2024]. See the Terms and Conditions (https://onlinelibrary.wiley.com/terms-and-conditions) on Wiley Online Library for rules of use; OA articles are governed by the applicable Creative Commons License

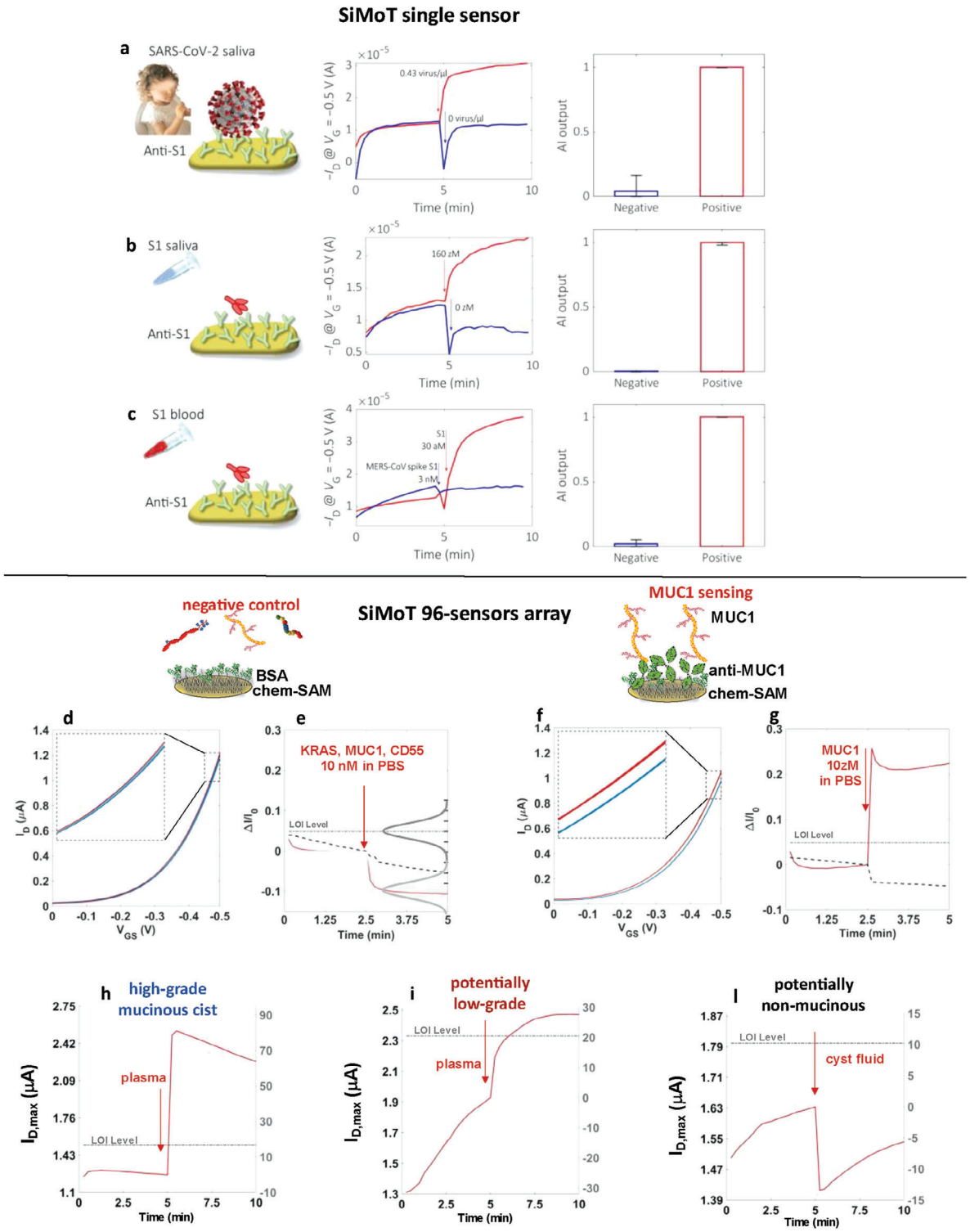

Figure 13. SiMoT single-sensor platform data and AI binary classifier output for the SARS-CoV-2 virus detected directly in the saliva of patients (a) and the Spike1 (S1) protein added both to saliva (b) and to blood (c) – see text for more details. Adapted and reproduced with permission from Ref. [13] Copyright 2022, AAAS under a Creative Commons Attribution-NonCommercial License 4.0 (CC BY-NC). SiMoT array data on the detection of the MUC1 protein marker. In panels (d,e) the negative control experiments transfer curves and current dynamics are shown while the same curves for the single molecule detection of MUC1 in PBS are shown in panels (f,g), respectively. In panels (h,i) and l) MUC1 detection from the plasma and the cyst fluids of patients in the presence of a high-grade mucinous cyst, potentially low-grade mucinous cyst, and potentially non-mucinous cyst, respectively – see text for more details Adapted and reproduced with permission from Ref. [8] Copyright 2023, Wiley-VCH under Creative Commons Attribution 4.0 License (CC BY 4.0).

© 2023 The Authors. Advanced Materials published by Wiley-VCH GmbH

15214095, 0, Downloaded from https://onlinelibrary.wiley.com/doi/10.1002/adma.202309705 by Universita Di Brescia, Wiley Online Library on [22/01/2024]. See the Terms and Conditions (https://onlinelibrary.wiley.com/terms-and-conditions) on Wiley Online Library for rules of use; OA articles are governed by the applicable Creative Commons License

elaborates on these standards through a set of criteria conveniently summarized with the acronym REASSURED.[56,128–130] Such an approach is under consideration also for better managing and cure of on non-infectious diseases.[129,130]

Nevertheless, the practical implementation of an approach focused on screening asymptomatic individuals is not yet considered mature, and it is facing criticism. This section reports on studies often utilizing data from the COVID-19 pandemic, providing evidence-based critical perspectives on the relevance and effectiveness of surveillance campaigns.[131–135] It is stated that the history of screening reflects situations where, in the best cases, there was potential for significant benefit, but at worst, it led to avoidable harm.[131] Moreover, one of the aspects that is most criticized is the suitability of the rapid antigen detection tests. Given the existing evidence, there is a lack of clarity concerning the efficacy of these devices in screening asymptomatic individuals to mitigate the transmission of a viral infection. Furthermore, there is an absence of evidence regarding their suitability for surveillance purposes. These studies call for better-performing POCT tests, particularly antigenic ones, and further appropriately powered trials to potentially revisit current recommendations.

In general, a correct methodological approach requires that the foundation of any screening initiative must originate from a targeted approach, addressing the unique aspects of each disease or condition and pivotal requisites are crucial for effective screening. Several aspects must be addressed the first one being the "validity of the test" which refers to the already introduced accuracy and precision of a diagnostic or screening test that must be able to measure what it is designed for. The "validity of the test" is an assessment of how well the test correctly identifies individuals with a particular condition (sensitivity) and excludes those without the condition (specificity). Validity is a crucial aspect of evaluating the overall reliability and effectiveness of a test in each context. High sensitivity indicates a low rate of false negatives, while high specificity indicates a low rate of false positives (**Section 4**) contributing to the overall validity of the test. A screening test's validity and reliability are paramount, demanding both high sensitivity in accurately detecting the disease and high specificity to minimize false positives. Another important aspect is to balance the benefits and the risks. Screening benefits, such as early detection and treatment, must demonstrably outweigh associated risks, encompassing psychological harm, overdiagnosis, and overtreatment. Finally, cost-effectiveness is to be addressed as screening programs must not only be effective but also economically sustainable, delivering substantial value for the invested resources. A comprehensive evaluation of the screening approach's efficacy and feasibility is indeed critically important to ensure its success and positive impact on public health. While certain aspects have been considered in the proposed technologies (diagnostic sensitivities and selectivities in preliminary pre-clinical studies as well as foreseen costs provided for SiMoT) it's important to emphasize that we are still in the early stages of developing POCT single-molecule technologies for early diagnosis. Consequently, most of the factors here recalled, intended to steer strategic directions throughout device development, are presently premature for systematic consideration.

8. Conclusion and Future Prospective

The surveillance of public health through the systematic screening of asymptomatic individuals across all living species is a visionary picture that, in principle, could be critically important for saving lives and optimizing the cost-effectiveness of healthcare systems. However, it is still not clearly demonstrated that such an approach can address several diseases including pandemic/epidemic outbreaks or progressive diseases, such as cancers, enabling early diagnosis. It is received that a surveillance campaign cannot be carried out without sufficiently highly performing and low-cost POCT technologies. Among these POCT options, strep tests or handheld reusable readers accompanied by appropriate disposable accessory cartridges are considered potentially extremely useful. However, the level of performance, particularly in terms of the high incidence of false-positive errors, is often insufficient to make them reliable for their intended scope.

Future availability of highly reliable and performing, small, disposable, easy-to-operate, fast, and affordable POCT holds the potential to change this scenario, opening a new era in which rapid and decentralized diagnostic capabilities transform healthcare delivery, facilitating timely interventions and improving patient outcomes. In this context, a couple of recently developed handheld POCT single-molecule technologies, the CRISPR lateral flow strip tests, combined with enzymatic amplification, and the SiMoT bioelectronic palmar devices, are reviewed. These technologies, which have reached technology readiness levels 5–6, are capable of single-molecule detections (at concentrations of 10^{-20} M in 0.1 mL) and exhibit quite high reliability (diagnostic sensitivity > 95–99%) which can further improve in the future. Moreover, they are multipurpose and hold high potential to be effectively utilized in resource-constrained settings.

In light of the great potential and the critical aspects here highlighted, a profound exploration of the present challenges and future perspectives is imperative for elevating POCT techniques capable of single-molecule reliable detections to a heightened level of technological readiness, particularly in the realm of early diagnosis. One of the primary challenges lies in ensuring the seamless integration and scalability of cutting-edge technologies into portable, user-friendly devices that can be readily deployed in diverse healthcare settings. The need for standardized protocols and robust quality control mechanisms is paramount to guarantee the accuracy and reliability of single-molecule POCT results. Additionally, issues related to affordability, accessibility, and equitable distribution of these advanced diagnostic tools demand careful consideration. Advancing these techniques requires collaborative efforts among interdisciplinary teams, bridging the gap between technology developers, clinicians, and regulatory bodies. Furthermore, addressing the dynamic landscape of infectious agents and emerging diseases necessitates constant innovation and adaptability in POCT methodologies. Enhancing the sensitivity and specificity of diagnostic assays, coupled with the ability to detect multiple analytes simultaneously, represents a pivotal direction for future advancements. Integration with digital health platforms and data analytics can further optimize the utility of POCT results for personalized patient care and population health management. Ethical considerations, such as

© 2023 The Authors. Advanced Materials published by Wiley-VCH GmbH

15214095, 0, Downloaded from https://onlinelibrary.wiley.com/doi/10.1002/adma.202309705 by Universita Di Brescia, Wiley Online Library on [22/01/2024]. See the Terms and Conditions (https://onlinelibrary.wiley.com/terms-and-conditions) on Wiley Online Library for rules of use; OA articles are governed by the applicable Creative Commons License

patient privacy and informed consent, must also be at the forefront of technological development. As we navigate the evolving landscape of early diagnosis through single-molecule POCT, a holistic approach that addresses technological, regulatory, ethical, and accessibility dimensions will be instrumental in realizing the full potential of these transformative diagnostic tools.

Acknowledgements

E.M. and F.T. contributed equally to this work as first authors L.T. acknowledges Eugenio Cantatore, Irene Esposito, Fabrizio Antonio Viola, and Mario Caironi for useful discussions. The following projects were acknowledged for partial financial support: The project BIOSCREEN (POR FESR 2014–2020, ID number 1831459, CUP E81B20000320007 funded by the European Commission, the Italian Government, and Regione Lombardia. H2020 – Electronic Smart Systems – SiMBiT: Single-molecule bio-electronic smart system array for clinical testing (Grant agreement ID: 824946). A binary sensor with single-molecule digit to discriminate biofluids enclosing zero or at least one biomarker (NoOne) ERC Starting Grant 2021 (GA 101040383); Tecnologie portatili e protocolli innovativi per la diagnosi ultrasensibile di Xylella fastidiosa direttamente in piante e vettori (1LIVEXYLELLA) Ministero dell'agricoltura, della sovranità alimentare e delle foreste – MIPAAF D.M. n.419161 del 13/09/2022; "I primi mille clinical trial con il Centro DIGITAL ASSAY", Centro di Innovazione Regionale Digital Assay, Presidente Prof. L. Torsi, Responsabile Scientifico UNIBA E. Macchia, Responsabile Scientifico UNIBS F.T., Regione PUGLIA Delibera Regionale n 702 del 08/11/2022, CUP B93C22000840001; Italian network of excellence for advanced diagnosis (INNOVA), Ministero della Salute -code PNC-E3-2022-23683266 PNC-HLS-DA, CUP: C43C22001630001; Complementary National Plan PNC-I.1 "Research initiatives for innovative technologies and pathways in the health and welfare sector" D.D. 931 of 06/06/2022, DARE – DigitAl lifelong pRevEntion initiative, code PNC0000002, CUP: B53C22006420001. PNRR MUR project PE0000023-NQSTI; MUR – Dipartimenti di Eccellenza 2023–2027 – Quantum Sensing and Modelling for One-Health (QuaSiModO). ChatGPT (https://chat.openai.com/) is acknowledged for suggesting improvements in the English form and the grammar.

Conflict of Interest

The authors declare no conflict of interest.

Keywords

clustered regularly interspaced short palindromic repeats/Cas (CRISPR/Cas), lateral flow strip test, one health, point of care testing (POCT), preventing healthcare, Single-molecule with a large transistor(SiMoT)

Received: September 19, 2023
Revised: November 20, 2023
Published online:

[1] R. Mayeux, *NeuroRx* **2004**, *1*, 182.
[2] S. Naylor, *Expert Rev. Mol. Diagn.* **2003**, *3*, 525.
[3] P. R. Srinivas, B. S. Kramer, S. Srivastava, *Lancet Oncol.* **2001**, *2*, 698.
[4] A. Shrivastava, T. Haase, T. Zeller, C. Schulte, *Front. Cardiovasc. Med.* **2020**, *7*, 601364.
[5] Y. Qu, J. Li, Q. Qin, D. Wang, J. Zhao, K. An, Z. Mao, Z. Min, Y. Xiong, J. Li, Z. Xue, *npj Parkinson's Dis.* **2023**, *9*, 18.
[6] T. K. Khan, D. L. Alkon, *J. Alzheimer's Dis.* **2015**, *44*, 729.
[7] J. D. Cohen, L. Li, Y. Wang, C. Thoburn, B. Afsari, L. Danilova, C. Douville, A. A. Javed, F. Wong, A. Mattox, R. H. Hruban, C. L. Wolfgang, M. G. Goggins, M. Dal Molin, T.-L. Wang, R. Roden, A. P. Klein, J. Ptak, L. Dobbyn, J. Schaefer, N. Silliman, M. Popoli, J. T. Vogelstein, J. D. Browne, R. E. Schoen, R. E. Brand, J. Tie, P. Gibbs, H.-L. Wong, A. S. Mansfield, et al., *Science* **2018**, *359*, 926.
[8] E. Genco, F. Modena, L. Sarcina, K. Björkström, C. Brunetti, M. Caironi, M. Caputo, V. M. Demartis, C. Di Franco, G. Frusconi, L. Haeberle, P. Larizza, M. T. Mancini, R. Österbacka, W. Reeves, G. Scamarcio, C. Scandurra, M. Wheeler, E. Cantatore, I. Esposito, E. Macchia, F. Torricelli, F. A. Viola, L. Torsi, *Adv. Mater.* **2023**, *35*, 2304102.
[9] X.-N. Shen, L.-D. Niu, Y.-J. Wang, X.-P. Cao, Q. Liu, L. Tan, C. Zhang, J.-T. Yu, *J. Neurol., Neurosurg. Psychiatry* **2019**, *90*, 590.
[10] N. Kandiah, S. H. Choi, C.-J. Hu, K. Ishii, K. Kasuga, V. C. T. Mok, *J. Alzheimer's Dis. Rep.* **2022**, *6*, 699.
[11] M. G. Krokidis, *AIMS Neurosci.* **2019**, *6*, 333.
[12] M. K. Bohn, G. Lippi, A. Horvath, S. Sethi, D. Koch, M. Ferrari, C.-B. Wang, N. Mancini, S. Steele, K. Adeli, *Clin. Chem. Lab. Med.* **2020**, *58*, 1037.
[13] E. Macchia, Z. M. Kovács-Vajna, D. Loconsole, L. Sarcina, M. Redolfi, M. Chironna, F. Torricelli, L. Torsi, *Sci. Adv.* **2022**, *8*, abo0881.
[14] S. H. Eshleman, L. Khaki, O. Laeyendecker, E. Piwowar-Manning, L. Johnson-Lewis, M. Husnik, B. Koblin, T. Coates, M. Chesney, A. Vallari, S. G. Devare, J. Hackett, *JAIDS, J. Acquired Immune Defic. Syndr.* **2009**, *52*, 121.
[15] S. K. Sailapu, E. Macchia, I. Merino-Jimenez, J. P. Esquivel, L. Sarcina, G. Scamarcio, S. D. Minteer, L. Torsi, N. Sabaté, *Biosens. Bioelectron.* **2020**, *156*, 112103.
[16] J. Merckx, R. Wali, I. Schiller, C. Caya, G. C. Gore, C. Chartrand, N. Dendukuri, J. Papenburg, *Ann. Intern. Med.* **2017**, *167*, 394.
[17] *EPPO Standards — Diagnostics. EPPO Bulletin*, **2019**, *49*, pp. 170–174, https://doi.org/10.1111/epp.12588.
[18] A. Armakolas, M. Kotsari, J. Koskinas, *Cancers* **2023**, *15*, 1579.
[19] C. Rolfo, A. Russo, *Nat. Rev. Clin. Oncol.* **2020**, *17*, 523.
[20] C. Alix-Panabières, *Nature* **2020**, *579*, S9.
[21] J. D. Cohen, A. A. Javed, C. Thoburn, F. Wong, J. Tie, P. Gibbs, C. M. Schmidt, M. T. Yip-Schneider, P. J. Allen, M. Schattner, R. E. Brand, A. D. Singhi, G. M. Petersen, S.-M. Hong, S. C. Kim, M. Falconi, C. Doglioni, M. J. Weiss, N. Ahuja, J. He, M. A. Makary, A. Maitra, S. M. Hanash, M. Dal Molin, Y. Wang, L. Li, J. Ptak, L. Dobbyn, J. Schaefer, N. Silliman, et al., *Proc. Natl. Acad. Sci. U. S. A.* **2017**, *114*, 10202.
[22] J. Kaiser, *Science* **2018**, *359*, 259.
[23] M. Ye, J. Wang, S. Pan, L. Zheng, Z.-W. Wang, X. Zhu, *Mol. Ther. Oncol.* **2022**, *24*, 101.
[24] C. Schulte, T. Barwari, A. Joshi, T. Zeller, M. Mayr, *Trends Mol. Med.* **2020**, *26*, 583.
[25] I. Palacín-Aliana, N. García-Romero, A. Asensi-Puig, J. Carrión-Navarro, V. González-Rumayor, Á. Ayuso-Sacido, *Biomedicines* **2021**, *9*, 906.
[26] S. N. Lone, S. Nisar, T. Masoodi, M. Singh, A. Rizwan, S. Hashem, W. El-Rifai, D. Bedognetti, S. K. Batra, M. Haris, A. A. Bhat, M. A. Macha, *Mol. Cancer* **2022**, *21*, 79.
[27] J. D. Cohen, A. A. Javed, C. Thoburn, F. Wong, J. Tie, P. Gibbs, C. M. Schmidt, M. T. Yip-Schneider, P. J. Allen, M. Schattner, R. E. Brand, A. D. Singhi, G. M. Petersen, S.-M. Hong, S. C. Kim, M. Falconi, C. Doglioni, M. J. Weiss, N. Ahuja, J. He, M. A. Makary, A. Maitra, S. M. Hanash, M. Dal Molin, Y. Wang, L. Li, J. Ptak, L. Dobbyn, J. Schaefer, N. Silliman, et al., *Proc. Natl. Acad. Sci. U. S. A.* **2017**, *114*, 10202.
[28] C. P. Mao, S. C. Wang, Y. P. Su, S. H. Tseng, L. He, A. A. Wu, R. B. S. Roden, J. Xiao, C. F. Hung, *Sci. Adv.* **2021**, *7*, eabg6522.
[29] E. Engvall, *Mol. Immunol.* **1971**, *8*, 871.
[30] H. A. Erlich, D. Gelfand, J. J. Sninsky, *Science* **1991**, *252*, 1643.

© 2023 The Authors. Advanced Materials published by Wiley-VCH GmbH

15214095, 0, Downloaded from https://onlinelibrary.wiley.com/doi/10.1002/adma.202309705 by Universita Di Brescia, Wiley Online Library on [22/01/2024]. See the Terms and Conditions (https://onlinelibrary.wiley.com/terms-and-conditions) on Wiley Online Library for rules of use; OA articles are governed by the applicable Creative Commons License

[31] H. Liu, Y. Lei, *Biosens. Bioelectron.* **2021**, *177*, 112901.
[32] D. M. Rissin, D. R. Walt, *Nano Lett.* **2006**, *6*, 520.
[33] D. R. Walt, *Anal. Chem.* **2013**, *85*, 1258.
[34] J. M. Rothberg, W. Hinz, T. M. Rearick, J. Schultz, W. Mileski, M. Davey, J. H. Leamon, K. Johnson, M. J. Milgrew, M. Edwards, J. Hoon, J. F. Simons, D. Marran, J. W. Myers, J. F. Davidson, A. Branting, J. R. Nobile, B. P. Puc, D. Light, T. A. Clark, M. Huber, J. T. Branciforte, I. B. Stoner, S. E. Cawley, M. Lyons, Y. Fu, N. Homer, M. Sedova, X. Miao, et al., *Nature* **2011**, *475*, 348.
[35] L. Zhang, C. Gu, H. Ma, L. Zhu, J. Wen, H. Xu, H. Liu, L. Li, *Anal. Bioanal. Chem.* **2019**, *411*, 21.
[36] M. Jinek, K. Chylinski, I. Fonfara, M. Hauer, J. A. Doudna, E. Charpentier, *Science* **2012**, *337*, 816.
[37] R. Aman, A. Mahas, M. Mahfouz, *ACS Synth. Biol.* **2020**, *9*, 1226.
[38] S. Gong, S. Zhang, F. Lu, W. Pan, N. Li, B. Tang, *Anal. Chem.* **2021**, *93*, 11899.
[39] F. Shao, J. S. Park, G. Zhao, K. Hsieh, T. H. Wang, *Anal. Chem.* **2023**, *95*, 3873.
[40] C. Qian, R. Wang, H. Wu, F. Zhang, J. Wu, L. Wang, *Anal. Chem.* **2019**, *91*, 11362.
[41] X. Wang, E. Xiong, T. Tian, M. Cheng, W. Lin, H. Wang, G. Zhang, J. Sun, X. Zhou, *ACS Nano* **2020**, *14*, 2497.
[42] T. Tian, B. Shu, Y. Jiang, M. Ye, L. Liu, Z. Guo, Z. Han, Z. Wang, X. Zhou, *ACS Nano* **2021**, *15*, 1167.
[43] D. Wang, X. Wang, F. Ye, J. Zou, J. Qu, X. Jiang, *ACS Nano* **2023**, *17*, 7250.
[44] N. E. Weckman, N. Ermann, R. Gutierrez, K. Chen, J. Graham, R. Tivony, A. Heron, U. F. Keyser, *ACS Sens.* **2019**, *4*, 2065.
[45] J. S. Park, K. Hsieh, L. Chen, A. Kaushik, A. Y. Trick, T. H. Wang, *Adv. Sci.* **2021**, *8*, 2003564.
[46] N. Atçeken, D. Yigci, B. Ozdalgic, S. Tasoglu, *Biosensors* **2022**, *12*, 1035.
[47] I. Santiago, *ChemBioChem* **2020**, *21*, 2880.
[48] R. Zhu, H. Jiang, C. Li, Y. Li, M. Peng, J. Wang, Q. Wu, C. Yan, Q. Bo, J. Wang, C. Shen, P. Qin, *Anal. Chim. Acta* **2023**, *1257*, 341175.
[49] E. Macchia, F. Torricelli, P. Bollella, L. Sarcina, A. Tricase, C. Di Franco, R. Österbacka, Z. M. Kovács-Vajna, G. Scamarcio, L. Torsi, *Chem. Rev.* **2022**, *122*, 4636.
[50] L. Sarcina, E. Macchia, G. Loconsole, G. D'attoma, P. Bollella, M. Catacchio, F. Leonetti, C. Di Franco, V. Elicio, G. Scamarcio, G. Palazzo, D. Boscia, P. Saldarelli, L. Torsi, *Adv. Sci.* **2022**, *9*, 2203900.
[51] E. Macchia, K. Manoli, B. Holzer, C. Di Franco, M. Ghittorelli, F. Torricelli, D. Alberga, G. F. Mangiatordi, G. Palazzo, G. Scamarcio, L. Torsi, *Nat. Commun.* **2018**, *9*, 3223.
[52] H. R. Boehringer, B. J. O'farrell, *Clin. Chem.* **2022**, *68*, 52.
[53] R. A. Smith, K. S. Andrews, D. Brooks, S. A. Fedewa, D. Manassaram-Baptiste, D. Saslow, O. W. Brawley, R. C. Wender, *CA Cancer J. Clin.* **2017**, *67*, 100.
[54] L. D. Wood, M. I. Canto, E. M. Jaffee, D. M. Simeone, *Gastroenterology* **2022**, *163*, 386.
[55] R. M. Witteles, S. Bokhari, T. Damy, P. M. Elliott, R. H. Falk, N. M. Fine, M. Gospodinova, L. Obici, C. Rapezzi, P. Garcia-Pavia, *JACC: Heart Failure* **2019**, *7*, 709.
[56] K. J. Land, D. I. Boeras, X.-S. Chen, A. R. Ramsay, R. W. Peeling, *Nat. Microbiol.* **2019**, *4*, 46.
[57] B. Das, J. Lou Franco, N. Logan, P. Balasubramanian, M. Il Kim, C. Cao, *Nanozymes in Point-of-Care Diagnosis: An Emerging Futuristic Approach for Biosensing*, Vol. *13*, Springer, Singapore, **2021**.
[58] E. Macchia, L. De Caro, F. Torricelli, C. D. Franco, G. F. Mangiatordi, G. Scamarcio, L. Torsi, *Adv. Sci.* **2022**, *9*, 2104381.
[59] Y. Lyu, L. An, H. Zeng, F. Zheng, J. Guo, P. Zhang, H. Yang, H. Li, *Talanta* **2023**, *260*, 124569.
[60] P. E. Sheehan, L. J. Whitman, *Nano Lett.* **2005**, *5*, 803.
[61] X. Wei, T. Penkauskas, J. E. Reiner, C. Kennard, M. J. Uline, Q. Wang, S. Li, A. Aksimentiev, J. W. F. Robertson, C. Liu, *ACS Nano* **2023**, *17*, 16369.
[62] Q. Zeng, X. Zhou, Y. Yang, Y. Sun, J. Wang, C. Zhai, J. Li, H. Yu, *Proc. Natl. Acad. Sci. U. S. A.* **2022**, *119*, 2120379119.
[63] *Impact of false-positives and false-negatives in the UK ' s COVID-19 RT-PCR testing programme*, https://www.gov.uk/government/publications (accessed: August 2023).
[64] S. Broeders, I. Huber, L. Grohmann, G. Berben, I. Taverniers, M. Mazzara, N. Roosens, D. Morisset, *Trends Food Sci. Technol.* **2014**, *37*, 115.
[65] M. Thompson, S. L. R. Ellison, R. Wood, *Pure Appl. Chem.* **2002**, *74*, 835.
[66] J. Mocak, A. M. Bond, S. Mitchell, G. Scollary, *Pure Appl. Chem.* **1997**, *69*, 297.
[67] P. Jing, H. Yi, S. Xue, R. Yuan, W. Xu, *RSC Adv.* **2015**, *5*, 65725.
[68] X. Bian, B. Guo, M. Zhao, D. Han, W. Cheng, F. Song, S. Ding, *ACS Appl. Mater. Interfaces* **2019**, *11*, 3715.
[69] M. Moretti, E. Di Fabrizio, S. Cabrini, R. Musetti, F. De Angelis, G. Firrao, *Biosens. Bioelectron.* **2008**, *24*, 141.
[70] OraQuick Rapid HIV Test, https://global.oraquick.com/why-oraquick (accessed: November 2023).
[71] Chembio's DPP HIV 1/2 Assay, https://chembio.com/products/dpp-hiv-12-assay-usa/ (accessed: November 2023).
[72] Clarity Strep A Test, https://claritydiagnostics.com/products/infectious-disease/clarity-strep-a-test-kit/ (accessed: November 2023).
[73] Real-time COVID-19 testing Cue, https://cuehealth.com/products/how-cue-detects-covid-19/ (accessed: November 2023).
[74] Biopix-t, https://biopix-t.com/products/ (accessed: November 2023).
[75] LumiraDx (US), https://www.lumiradx.com/us-en/instrument (accessed: November 2023).
[76] Alere BinaxNOW Influenza Test, https://www.globalpointofcare.abbott/us/en/product-details/binaxnow-influenza-a-and-b-2.html (accessed: November 2023).
[77] A. ID Now, https://www.globalpointofcare.abbott/gb/en/product-details/id-now.html (accessed: November 2023).
[78] *Quantum MDx Q POC*, https://www.quantumdx.com/ (accessed: November 2023).
[79] Pluslife, https://www.pluslife.com/ (accessed: November 2023).
[80] *SR-XTM SIMOA Quanterix*, https://www.quanterix.com/instruments/quanterix-sr-x/ (accessed: November 2023).
[81] C. GeneXpert, https://www.cepheid.com/en-US/systems/genexpert-family-of-systems/genexpert-xpress.html (accessed: November 2023).
[82] *Thermo ABI QuantStudio DX Real-Time PCR 4470660 – AV*, https://www.bostonind.com/ (accessed: November 2023).
[83] L. Cohen, D. R. Walt, *Annu. Rev. Anal. Chem.* **2017**, *10*, 345.
[84] D. M. Rissin, C. W. Kan, T. G. Campbell, S. C. Howes, D. R. Fournier, L. Song, T. Piech, P. P. Patel, L. Chang, A. J. Rivnak, E. P. Ferrell, J. D. Randall, G. K. Provuncher, D. R. Walt, D. C. Duffy, *Nat. Biotechnol.* **2010**, *28*, 595.
[85] *SP-X Imaging and Analysis SystemTM Quanterix*, https://www.quanterix.com/instruments/the-sp-x-imaging-and-analysis-system/ (accessed: November 2023).
[86] C. Scandurra, K. Björkström, L. Sarcina, A. Imbriano, C. Di Franco, R. Österbacka, P. Bollella, G. Scamarcio, L. Torsi, E. Macchia, *Adv. Mater. Technol.* **2023**, 2201910.
[87] G. Salazar, M. N. Russi-Vigoya, *Ergonomics Des.* **2021**, *29*, 25.
[88] J. P. Broughton, X. Deng, G. Yu, C. L. Fasching, V. Servellita, J. Singh, X. Miao, J. A. Streithorst, A. Granados, A. Sotomayor-Gonzalez, K. Zorn, A. Gopez, E. Hsu, W. Gu, S. Miller, C.-Y. Pan, H. Guevara, D. A. Wadford, J. S. Chen, C. Y. Chiu, *Nat. Biotechnol.* **2020**, *38*, 870.

© 2023 The Authors. Advanced Materials published by Wiley-VCH GmbH

15214095, 0, Downloaded from https://onlinelibrary.wiley.com/doi/10.1002/adma.202309705 by Universita Di Brescia, Wiley Online Library on [22/01/2024]. See the Terms and Conditions (https://onlinelibrary.wiley.com/terms-and-conditions) on Wiley Online Library for rules of use; OA articles are governed by the applicable Creative Commons License

[89] K. Guk, J. O. Keem, S. G. Hwang, H. Kim, T. Kang, E.-K. Lim, J. Jung, *Biosens. Bioelectron.* **2017**, *95*, 67.
[90] E. Macchia, K. Manoli, B. Holzer, C. Di Franco, R. A. Picca, N. Cioffi, G. Scamarcio, G. Palazzo, L. Torsi, *Anal. Bioanal. Chem.* **2019**, *411*, 4899.
[91] C. Scandurra, K. Björkström, L. Sarcina, A. Imbriano, C. Di Franco, R. Österbacka, P. Bolella, G. Scamarcio, L. Torsi, E. Macchia, *Adv. Mater. Technol.* **2023**, *8*, 2201910.
[92] E. Macchia, A. Tiwari, K. Manoli, B. Holzer, N. Ditaranto, R. A. Picca, N. Cioffi, C. Di Franco, G. Scamarcio, G. Palazzo, L. Torsi, *Chem. Mater.* **2019**, *31*, 6476.
[93] E. Macchia, L. Sarcina, R. A. Picca, K. Manoli, C. Di Franco, G. Scamarcio, L. Torsi, *Anal. Bioanal. Chem.* **2020**, *412*, 811.
[94] E. Macchia, K. Manoli, C. Di Franco, R. A. Picca, R. Österbacka, G. Palazzo, F. Torricelli, G. Scamarcio, L. Torsi, *ACS Sens.* **2020**, *5*, 1822.
[95] J. E. Van Dongen, J. T. W. Berendsen, R. D. M. Steenbergen, R. M. F. Wolthuis, J. C. T. Eijkel, L. I. Segerink, *Biosens. Bioelectron.* **2020**, *166*, 112445.
[96] Z. O. Uygun, L. Yeniay, F. Gi?Rgi?N Sagin, *Anal. Chim. Acta* **2020**, *1121*, 35.
[97] R. Hajian, S. Balderston, T. Tran, T. Deboer, J. Etienne, M. Sandhu, N. A. Wauford, J.-Y. Chung, J. Nokes, M. Athaiya, J. Paredes, R. Peytavi, B. Goldsmith, N. Murthy, I. M. Conboy, K. Aran, *Nat. Biomed. Eng.* **2019**, *3*, 427.
[98] W. Xu, T. Jin, Y. Dai, C. C. Liu, *Biosens. Bioelectron.* **2020**, *155*, 112100.
[99] R. Pu, S. Liu, X. Ren, D. Shi, Y. Ba, Y. Huo, W. Zhang, L. Ma, Y. Liu, Y. Yang, N. Cheng, *J. Virol. Methods* **2022**, *300*, 114392.
[100] M. Wang, R. Zhang, J. Li, *Biosens. Bioelectron.* **2020**, *165*, 112430.
[101] A. Ramachandran, J. G. Santiago, *Anal. Chem.* **2021**, *93*, 7456.
[102] Z. Han, F. Wan, J. Deng, J. Zhao, Y. Li, Y. Yang, Q. Jiang, B. Ding, C. Liu, B. Dai, J. Sun, *Nano Today* **2021**, *38*, 101203.
[103] Y. Li, J. Deng, Z. Han, C. Liu, F. Tian, R. Xu, D. Han, S. Zhang, J. Sun, *J. Am. Chem. Soc.* **2021**, *143*, 1290.
[104] H. Zhang, Y. Xu, Z. Fohlerova, H. Chang, C. Iliescu, P. Neuzil, *TrAC, Trends Anal. Chem.* **2019**, *113*, 44.
[105] J. P. Broughton, X. Deng, G. Yu, C. L. Fasching, V. Servellita, J. Singh, X. Miao, J. A. Streithorst, A. Granados, A. Sotomayor-Gonzalez, K. Zorn, A. Gopez, E. Hsu, W. Gu, S. Miller, C.-Y. Pan, H. Guevara, D. A. Wadford, J. S. Chen, C. Y. Chiu, *Nat. Biotechnol.* **2020**, *38*, 870.
[106] L. Becherer, N. Borst, M. Bakheit, S. Frischmann, R. Zengerle, F. Von Stetten, *Anal. Methods* **2020**, *12*, 717.
[107] E. A. Pumford, J. Lu, I. Spaczai, M. E. Prasetyo, E. M. Zheng, H. Zhang, D. T. Kamei, *Biosens. Bioelectron.* **2020**, *170*, 112674.
[108] I. M. Lobato, C. K. O'sullivan, *TrAC, Trends Anal. Chem.* **2018**, *98*, 19.
[109] M. A. Cobzariu, M. J. Lobo-Castanon, R. Miranda-Castro, *Curr. Opin. Electrochem.* **2023**, *40*, 101322.
[110] R. Paul, E. Ostermann, Q. Wei, *Biosens. Bioelectron.* **2020**, *169*, 112592.
[111] B. Koo, D.-E. Kim, J. Kweon, C. E. Jin, S.-H. Kim, Y. Kim, Y. Shin, *Sens. Actuators, B* **2018**, *273*, 316.
[112] M. Liang, Z. Li, W. Wang, J. Liu, L. Liu, G. Zhu, L. Karthik, M. Wang, K. F. Wang, Z. Wang, J. Yu, Y. Shuai, J. Yu, L. Zhang, Z. Yang, C. Li, Q. Zhang, T. Shi, L. Zhou, F. Xie, H. Dai, X. Liu, J. Zhang, G. Liu, Y. Zhuo, B. Zhang, C. Liu, S. Li, X. Xia, Y. Tong, et al., *Nat. Commun.* **2019**, *10*, 3672.
[113] L. Sarcina, F. Viola, F. Modena, R. A. Picca, P. Bollella, C. Di Franco, N. Cioffi, M. Caironi, R. Österbacka, I. Esposito, G. Scamarcio, L. Torsi, F. Torricelli, E. Macchia, *Anal. Bioanal. Chem.* **2022**, *414*, 5657.
[114] C. Di Franco, E. Macchia, L. Sarcina, N. Ditaranto, A. Khaliq, L. Torsi, G. Scamarcio, *Adv. Mater. Interfaces* **2022**, *10*, 2201829.
[115] L. Kergoat, L. Herlogsson, D. Braga, B. Piro, M.-C. Pham, X. Crispin, M. Berggren, G. Horowitz, *Adv. Mater.* **2010**, *22*, 2565.
[116] P. Oliveri, *Anal. Chim. Acta* **2017**, *982*, 9.
[117] S. Jain, M. Nehra, R. Kumar, N. Dilbaghi, T. Hu, S. Kumar, A. Kaushik, C.-Z. Li, *Biosens. Bioelectron.* **2021**, *179*, 113074.
[118] F. M. Shimizu, A. de Barros, M. L. Braunger, G. Gaal, A. Riul, *TrAC, Trends Anal. Chem.* **2023**, *165*, 117115.
[119] P. Geladi, J. Linderholm, In *Comprehensive Chemometrics (Second Edition)* (Eds.: S. Brown, R. Tauler, B. Walczak), Elsevier, Oxford, **2020**, pp. 17–37.
[120] B. K. Lavine, W. S. Rayens, *3.27 – Classification: Basic Concepts*, 2nd edn., Vol. *3*, Elsevier, Amsterdam **2020**.
[121] P. Oliveri, G. Downey, *TrAC, Trends Anal. Chem.* **2012**, *35*, 74.
[122] R. G. Brereton, *J. Chemom.* **2011**, *25*, 225.
[123] A. Retico, I. Gori, A. Giuliano, F. Muratori, S. Calderoni, *Front. Neurosci.* **2016**, *10*, 306.
[124] I. Irigoien, B. Sierra, C. Arenas, *Sci. World J.* **2014**, *2014*, 730712.
[125] M. Barker, W. Rayens, *J. Chemom.* **2003**, *17*, 166.
[126] R. A. Fisher, *Ann. Hum. Genet.* **1936**, *7*, 179.
[127] S. Geisser, *J R Stat Soc Series B Stat Methodol* **1964**, *26*, 69.
[128] M. Naseri, Z. M. Ziora, G. P. Simon, W. Batchelor, *Rev. Med. Virol.* **2022**, *32*, e2263.
[129] T. Bhardwaj, L. N. Ramana, T. K. Sharma, *Current Advancements and Future Road Map to Develop ASSURED Microfluidic Biosensors for Infectious and Non-Infectious Diseases*, Vol. *12*, Biosensors, Anyang, Korea **2022**.
[130] J. H. Zafra-Tanaka, D. Beran, B. Vetter, R. Sampath, A. Bernabe-Ortiz, *J. Diabetes Sci. Technol.* **2022**, *16*, 962.
[131] J. P. Skittrall, M. D. Fortune, H. Jalal, H. Zhang, D. A. Enoch, N. M. Brown, A. Swift, *Asymptomatic testing for SARS-CoV-2 needs clear goals and protocols*, Vol. *1*, Elsevier, Amsterdam **2021**.
[132] M. Döhla, C. Boesecke, B. Schulte, C. Diegmann, E. Sib, E. Richter, M. Eschbach-Bludau, S. Aldabbagh, B. Marx, A.-M. Eis-Hübinger, R. M. Schmithausen, H. Streeck, *Public Health* **2020**, *182*, 170.
[133] M. Ryan, *Advice to NPHET-Evidence summary for use of rapid antigen testing for screening or surveillance of asymptomatic individuals to limit transmission of SARS-CoV-2 Health Information and Quality Authority*, **2021**.
[134] H. E. Bloomfield, A. Olson, N. Greer, A. Cantor, R. Macdonald, I. Rutks, T. J. Wilt, *Ann. Intern. Med.* **2014**, *161*, 46.
[135] O. F. Clerc, T. A. Fuchs, J. Stehli, D. C. Benz, C. Gräni, M. Messerli, A. A. Giannopoulos, R. R. Buechel, T. F. Lüscher, A. P. Pazhenkottil, P. A. Kaufmann, O. Gaemperli, *Eur. Heart J.: Cardiovasc. Imaging* **2018**, *19*, 838.
[136] T. J. Sullivan, A. K. Dhar, R. Cruz-Flores, A. G. Bodnar, *Sci. Rep.* **2019**, *9*, 19702.

© 2023 The Authors. Advanced Materials published by Wiley-VCH GmbH

15214095, 0, Downloaded from https://onlinelibrary.wiley.com/doi/10.1002/adma.202309705 by Universita Di Brescia, Wiley Online Library on [22/01/2024]. See the Terms and Conditions (https://onlinelibrary.wiley.com/terms-and-conditions) on Wiley Online Library for rules of use; OA articles are governed by the applicable Creative Commons License

Luisa Torsi is a professor of chemistry at the University of Bari and president of the Centre on Single-Molecule Digital Assay. She is also a member of the Accademia dei Lincei. Torsi has been awarded the H.E. Merck prize and the Wilhelm Exner Medal. She was also the only woman president of the European Material Research Society. Torsi has authored ≈230 papers that collected over 16 200 Google Scholar citations resulting in an h-index of 63. Gathered research funding for over 40 M€, comprises several European, national, and regional projects. Torsi is committed to role-modeling for younger women scientists.

© 2023 The Authors. Advanced Materials published by Wiley-VCH GmbH

15214095, 0, Downloaded from https://onlinelibrary.wiley.com/doi/10.1002/adma.202309705 by Universita Di Brescia, Wiley Online Library on [22/01/2024]. See the Terms and Conditions (https://onlinelibrary.wiley.com/terms-and-conditions) on Wiley Online Library for rules of use; OA articles are governed by the applicable Creative Commons License